(NASA-CR-149108) SUPPORTING STUDIES IN CLOUD IMAGE PROCESSING FOR PLANETARY FLYBYS OF THE 1970'S Semiannual Progress Report, 1 Jan. - 30 Jun. 1975 (Wisconsin Univ.) 64 p
N77-70808
Unclas
00/98 08031

SUPPORTING STUDIES IN CLOUD IMAGE PROCESSING FOR PLANETARY FLYBYS OF THE 1970'S

Semi-Annual Progress Report
on
NASA Grant NGR 50-002-189

for the period
1 January 1975 through 30 June 1975

Principal Investigator: V. E. Suomi
Program Manager: R. J. Krauss

Space Science and Engineering Center
University of Wisconsin-Madison
1225 West Dayton Street
Madison, Wisconsin 53706

PRESENT PROGRAM STATUS

We will first report briefly on recent work performed at the University of Wisconsin on the Mariner 10 Venus flyby data on NASA Grant NGR 50-002-189 and then detail our present plans for extracting cloud motions from the high resolution image data. It is apparent after a year's work that added effort could be very productive in improving our quantitative knowledge of Venus. We intend to further analyze these images using our Man-computer Interactive Data Access System (McIDAS).

The wealth of quantitative information contained in the Mariner 10 images has considerably exceeded our estimates. We have been able to determine large scale structure of the global wind field, but there are numerous other smaller features in the data as well. These additional features require more care to analyze because there is such an abundance of structure on different time and space scales which must be carefully sorted out. What this structure indicates could be extremely important. For example, we have identified a few cases of vertical wind shear. Vertical wind shear is quantitatively related to the horizontal temperature gradient. Such indirect information is potentially very valuable for understanding energy balance and dynamics.

At the GISS conference last October 15, V. E. Suomi reported early results of our global wind field analysis. A more detailed paper is in preparation for submission to the Journal of Atmospheric Sciences. A draft copy is enclosed as Appendix A. At least another year's effort will be needed to fully extract quantitative results from the Venus data, however. The MVM mission was our first attempt to apply sophisticated meteorological analysis tools to data from a Mariner type TV imaging system. Much effort (some of it funded by this grant and some through JPL) had to be directed to preparing

the data base and adapting existing meteorological image analysis techniques to the Venus clouds, which have low contrast compared to Earth clouds. We have now learned how to go about this, and because we were successful in obtaining the global wind field in one case we can begin to analyze more data.

We are reasonably confident at this time of the existence of a vortex structure in the upper atmosphere wind field, with a velocity maximum in the mid-latitudes. A transition occurs there with the zonal flow changing from a condition of nearly constant angular momentum at low latitudes to nearly constant angular velocity at high latitudes. As a result, one ought to expect variations in the lower atmosphere as a function of latitude. This expectation has had an impact on another NASA program: A presentation of our results was made to the atmospherics subgroup of the Pioneer Venus program in March in an effort to initiate retargeting of at least one of the small probes to a latitude above 45 degrees. The significance of the mid-latitude region was appreciated by the other scientists, and with their support, we succeeded in getting the Pioneer project to change the targeting area for one of the small probes.

In the meantime, while data analysis continued at SSEC, Professor Suomi communicated the measurement results to other scientific groups in talks at:

Meteorological Service	Budapest	15 November 1974
National Accelerator Lab	Batavia	15 January 1975
American Assn. for the Advancement of Science	Washington, D.C.	30 January 1975
Applied Physics Lab	Silver Springs	31 January 1975
Meteorological Institute	Berlin	5 March 1975

with a generally favorable reception.

The meridional structure of the zonal motion field implies meridional motion away from the equator and a tendency to conserve angular momentum on the equatorward side of the polar ring. A mean meridional velocity of -2 ± 5 m/s is measured in the southern hemisphere. Also seen is a tendency toward zonal acceleration in the equatorial region $\pm 30°$, these motions imply horizontal velocity divergence and require upward mass flow. Such flow is related to the drive for the zonal winds. The conceptual picture presented was that of a modified Hadley cell. We have been able to measure a zonal retrograde flow of ~95 m/s at the equator, increasing to 120 m/s at 45 degrees latitude and then sharply decreasing toward even higher latitudes.

Additional analysis has shown that weak meridional motions flow from equator to pole in each hemisphere. A model is being developed which may explain the shape of the spiral streaks on Venus as a function of the measured zonal and meridional velocities. We have also observed zonal acceleration over a wide area on the sunlit side of the planet, but because of a target selection bias due to spacecraft/planet viewing geometry, an exact magnitude cannot be determined without greatly improved statistics.

In addition to using the overlapping pictures to give us local relative motion, we will eventually be able to do "leap frog" navigation from the reference points on the limb in one frame to the Venus disk center in another frame, so local global motion fields can be related to each other. This is a complicated procedure, however, and will take some time to develop.

The Venus image data library at Wisconsin is nearly complete. The Mariner 10 Venus data tapes at Jet Propulsion Laboratory were duplicated starting in July, 1974, and were shipped to SSEC for analysis. Over 500 tapes are now catalogued and indexed with an additional 50 scheduled to

arrive before the end of June 1975. This collection of digital Venus image data is the only complete set outside of JPL and will receive extended use by us over the next few years. The reasons for this are: (1) the tapes can be quantitatively analyzed using our McIDAS system, and (2) the time and space resolution of the data set is significantly different from any other data set (existing or planned) because it covers so wide a range of time and space scales. Consequently, this Mariner 10 Venus data is likely to remain unique for the next 10-15 years.

We will be able to extract more information from tapes than from hard copy images because tapes contain time sequenced data with the full photometric and geometric resolution obtained by the TV camera. The overlapped portions of the images are, in fact, the most important part of the data. This is the part trimmed away in hard copy mosaics! McIDAS was developed at SSEC to analyze strings of digital earth satellite data in the time domain. It is a unique analysis system in that it combines digital precision, analog speed and bandwidth, and guiding human intelligence in a mix optimized for meteorological analysis. Using McIDAS, we will be able to look at subtle effects and time variations impossible to obtain from hard copy.

The tape data base has a spatial resolution of 300 meters to 100 kilometers, and a time resolution of 42 seconds to 8 days. The tapes therefore contain information about atmospheric motions on Venus at all scales, from organized global circulation to scale height size turbulence. None of the high resolution images have yet been analyzed for dynamic information content, but we hope to start as soon as the proper navigation tools are ready.

Existing funding from the Mariner Venus/Mercury project will carry our current effort through October or November 1975. We are asking for additional support to continue Venus data analysis to the end of June, 1976. The tasks will require approximately one man year of SSEC staff effort during the 8 month period, plus technical help, one graduate student, and computer support. We are confident that the scientific yield from these "old" Venus pictures will exceed what has been extracted so far.

PROPOSED FUTURE WORK

We propose three areas of work for the next year:

1. A Search for Local Phenomena - The high resolution images offer an opportunity to look for (a) changes in cloud shape, (b) vertical wind shear, (c) local turbulence or convection, (d) small or large scale gravity waves, (e) dynamic instabilities, (f) changes in cloud thickness, and (g) changes in UV absorber concentration.

2. Energy and Momentum Transport Mechanisms - The circulation in the stratosphere of Venus shows evidence of several types of wave motion or periodic disturbances, as evidenced by the variations of large scale cloud features. Examples are the appearance of the bowlike waves, the cross-equatorial motion of the circumequatorial belts, the meridional wobble of the polar ring, the intensity modulation of the Y and Ψ features, and the periodicity and organization of cloud features in low latitudes. We have measured the cloud motions, corresponding to mass transport, but to completely specify the general circulation in the upper atmosphere it is necessary to determine energy and momentum transport as well.

We propose to extend our analysis of large scale motions to the full 8 days of Mariner 10 observations. These should be related to ground based

observations as well. With this information, it should be possible to test some of the assumptions underlying existing general circulation models.

3. Venus Movie - We have been experimenting with the use of McIDAS for communication of results as well as for analysis. The TV medium is a very powerful tool for accessing the time domain. We recently generated a demonstration videotape and 16 mm film at SSEC and found the result satisfactory and worth pursuing further. The final version will contain the full disk images of Venus in motion plus closeups of smaller dynamic phenomena found in the high resolution images. This would take full advantage of the data organization and "leap frog" navigation techniques, and communicate the results of our analysis to the scientific community and the general public in a more understandable and dynamic way than still pictures. Such a movie would serve a useful pedagogical purpose in pointing out features important to atmospheric analysis from images.

APPENDIX A

UV Cloud Motions on Venus from Mariner 10 Images

Robert J. Krauss

ABSTRACT

A synoptic scale wind field has been measured in the stratosphere of Venus by observation of the motion of 100-300 km size UV cloud features in four Mariner 10 TV images. The cloud features are estimated to lie primarily in the 60-70 km altitude range. The UV images have an effective wavelength of 355 nm, cover a time interval of 3 1/2 hours, and were made about 2 1/2 days after Venus encounter. Major features of the wind field include: a) a vortex structure in each hemisphere with probable widespread upwelling at low latitudes and convergence at the poles; b) an equatorial zonal velocity of - 92 $\pm$ 7 m/s increasing to - 120 $\pm$ 10 m/s near 45° latitude; c) a mean meridional velocity gradient of 0.12 m/s/deg; d) a widespread longitudinal velocity gradient comparable to the meridional gradient in magnitude and observed at all latitudes below 60°; e) vertical wind shear in the zonal flow at low latitudes, with a mean value of 10-15 m/s rms. Considerable space is devoted to summarizing previous data in a dynamical context, and to explaining the measuring process and analysis techniques before full details of the measurements are presented.

(Note: Pictures for Figure 10 were not available at this time and have been omitted.)

UV Cloud Motions on Venus from Mariner 10 Images

Robert J. Krauss

ABSTRACT

A synoptic scale wind field has been measured in the stratosphere of Venus by observation of the motion of 100-300 km size UV cloud features in four Mariner 10 TV images. The cloud features are estimated to lie primarily in the 60-70 km altitude range. The UV images have an effective wavelength of 355 nm, cover a time interval of 3 1/2 hours, and were made about 2 1/2 days after Venus encounter. Major features of the wind field include: a) a vortex structure in each hemisphere with probable widespread upwelling at low latitudes and convergence at the poles; b) an equatorial zonal velocity of -92 ± 7 m/s increasing to -120 ± 10 m/s near 45° latitude; c) a mean meridional velocity gradient of 0.12 m/s/deg; d) a widespread longitudinal velocity gradient comparable to the meridional gradient in magnitude and observed at all latitudes below 60°; e) vertical wind shear in the zonal flow at low latitudes, with a mean value of 10-15 m/s rms. Considerable space is devoted to summarizing previous data in a dynamical context, and to explaining the measuring process and analysis techniques before full details of the measurements are presented.

CONTENTS

I. INTRODUCTION

A planetary atmosphere radiatively heated at the equator and cooled at the poles must transport heat poleward to maintain its global energy balance and relieve sun induced pressure gradients. A stringent dynamical contraint is also imposed on the resulting mass flow. There will be a need to conserve angular momentum. In addition, pressure induced motions will be distributed zonally, meridionally, and vertically by friction and dynamically induced shear. Thus, any physically complete atmospheric model must be a three dimensional system with a dynamic balance of mass, energy, and momentum. Even though these conditions strongly limit the range of possibilities for models of the circulation, any planetary atmosphere is structurally complex enough, to have many unknown quantities remaining. Observations of atmospheric motions on a global scale provide a useful additional constraint on such models. Motions of the UV markings measured in the Mariner 10 flyby images of Venus were first reported by Murray, et.al. (1974). Figure 1 (from the report) illustrates the major global scale features on Venus and nomenclature. Additional observations using the Mariner 10 images are reported here, based on tracking edge detail and light and dark features of 100-300 km scale size in four Mariner 10 TV images with 15 km/pixel resolution. The total time interval was about 3 1/2 hours.

Before the techniques and measurements are presented, however, it should be made clear just what is being measured. The subject of the Venus clouds has been a long standing and many-sided controversy, often surrounded by confusion. Full understanding of the data requires the proper conceptual framework, which is lacking at the present time. It is unlikely that all the data assembled to date can be properly interpreted until we gain better understanding of vertical structure, atmospheric chemistry, and the general circulation. Such knowledge can be gained from atmospheric probes and from long time base observations of the cloud motions. The Pioneer Venus mission in 1978 will help greatly in this regard. There have, however, been a few commonly accepted pieces of evidence which are well established. Coupled with new observations from Mariner 10, those established facts can be used as a basis to interpret the motions of the UV markings and to provide fresh insight, if not full understanding. So we will first review some of the evidence, with emphasis on dynamical features of the atmosphere and how they might be related to the UV markings.

The solid surface of Venus has never been reliably seen, and its high albedo led many astronomers to conclude that Venus was completely cloud covered. The Mariner 10 pictures have shown this to be true. Through the orange filter, Venus appears to be a diffuse and featureless ball of fog, though very faint large scale contrasts can occasionally be seen (Murray, et.al. 1974) which generally correlate with the more distinct large scale UV contrasts (Hapke, 1975). In blue light, the same large scale features have slightly greater contrast than in orange but there is a more definite threshold near 400 nm (Coffeen, 1971). Many additional small scale details ~100 km, begin to show up in the Mariner 10 UV images with contrasts of 5-10%. This contrast threshold in the UV has led many observers to conclude that the Venus clouds contain a UV absorber, since it is difficult to explain such a sharp contrast change in terms of physical cloud structure alone.

Travis (1975) and Hapke (1975) review the cloud contrast problem in terms of recent evidence and discuss various models.

The diffuse haze structure of the clouds seems well established, however. Hapke (1975) and Deveaux (1974) find that at all wavelengths of the Mariner 10 images the clouds act like isotropic scatterers characteristic of a deep homogeneous scattering medium. Detailed analysis of earth based polarization measurements (Hansen and Hovenier, 1974) supports this structural picture and places some hard quantitative limits on: (a) particle shape - spherical and therefore probably liquid; (b) effective radius 1.05 $\pm$ 0.10 μm with a narrow size distribution of 0.07 $\pm$ 0.02 μm effective variance; and, (c) visual refractive index 1.44 $\pm$ 0.015 with a normal dispersion curve. A strong electrolyte solution could form such a fine liquid aerosol at the existing temperatures and vapor pressures. Only one - sulfuric acid - has the proper refractive index and satisfies other observational evidence (Young, 1973, 1975, Pollack et.al., 1975).

The mean pressure at which scattered light is observed in the polarization observations is ~50 mb (Hansen and Hovenier, 1974), and corresponds to approximately the $\tau = 1$ optical depth and about 65-70 km altitude when looking vertically into this aerosol haze. Estimates of particle density yield 30-40 droplets per cubic centimeter (from observed mixing ratios), so visibility at this altitude is more like a hazy day in Los Angeles. We are not observing a dense fog or Earthlike cumulus type clouds.

O'Leary (1975) measured the limb haze layer in the Mariner 10 images at approximately 80 km altitude (~5 mb) and found a scale height of 1.5 km, whereas he got a scale height for the underlying haze of 2.5-3 km. Neither O'Leary nor Murray, et.al. (1974) saw any horizontal variation of the 5 mb haze in the Mariner 10 pictures on the scale of the UV marking details we have measured. The 5 mb haze layer seems horizontally uniform on a scale of 1000 km or more, while we report here on tracking of cloud elements of 100-300 km which are clearly contrasted with their surroundings. If the 5 mb haze contained the UV markings, the markings ought to have been visible in the Mariner 10 limb pictures. The UV markings must therefore be lower than 5 mb (80 km). If one assumes that the UV absorber is vertically distributed rather than concentrated in a thin horizontal layer, that is, if the absorber is subject to the same transport conditions as the rest of the surrounding atmosphere, then it is likely the UV markings are substantially lower than 80 km. They would be below 70 km, for it would not be possible to produce the observed 5-10% contrast variations at 75 km ($\tau \approx 2$) without getting variations as well from still visible portions of the atmosphere near 60-65 km, ($\tau \approx 3$-4) for example. If the markings are restricted to a very thin altitude layer, however, we can only say that they are above 60 km, the lower limit of visibility in the haze.

Spectroscopic studies of absorption on Venus in the near IR (Young, 1972) provide valuable information on gas concentration, temperature and pressure. Such absorption lines are formed lower in the atmosphere, around 100-200 mb (60-65 km), since the effective reflecting layer for longer wavelengths is lower in the hazy atmosphere. Surprisingly, the amount of CO_2 above this reflecting layer varies by as much a factor of 2 from day to day, corresponding to a large scale organized vertical motion of ~3 km in the reflecting layer or a change of 50-100% in the gas concentration above the reflecting layer

if the layer remains at constant altitude.

Water vapor, on the other hand, has been observed to vary locally across the disk of Venus, and in concentrations ranging over 2 orders of magnitude (Young, 1975; Barker, 1975). While the haze cannot be water drops or ice, it is possible that the water vapor is somehow related to small scale atmospheric activity such as the observed convective cells (Murray, et.al., 1974), while the CO_2 variations are related to global scale mass motions or waves. The important fact is that there is temporally varying activity between 100-200 mb on the same spatial scales as we see details in the Venus UV clouds. The scattered effective temperatures clustering around 250° $\pm$ 10°K are also consistent with some vertical and horizontal inhomogeneity at these altitudes.

Traub and Carlton (1975), have investigated Doppler shifts in the near IR spectral features and find a mean retrograde mass motion of 83 $\pm$ 10 m/s at the equator, with a tendency for higher velocities at the evening terminator. Meridional motion, if it exists, is smaller, and the direction somewhat less conclusive. Since the velocities were measured at widely varying times, much of the scatter might be real; and since these are absorption lines, it is hard to ascribe the Doppler shifts to anything but mass motion of CO_2. Traub and Carlton review ground based measurements of the large scale UV markings, which also show ~100 m/s zonal motion and a tendency to accelerate from morning to evening. The total picture of the spectroscopic studies indicates that the UV features in the Mariner 10 images are embedded in a fast zonal mass flow exhibiting dynamic variations over a wide variety of time and space scales.

Going still lower in the atmosphere, we note that the minimum observable contrast the Mariner 10 TV cameras can resolve is ~1/2%, so that even if the UV markings had 100% contrast and were buried deep in the haze, we could not see them below $\tau = 5$. For moderate contrasts, it seems unlikely, with a haze scale height of 2.5-4 km, that we are looking at cloud features below 60 km altitude, although the possibility of holes in the clouds remains.

Lacis (1975) has placed a number of the upper atmosphere observations on a convenient diagram (Figure 2), showing that there is probably a discontinuity in aerosol scale height above 50 mb, in agreement with the findings of O'Leary (1975). This transition may conceivably vary in height from time to time, but its presence could well indicate a change in the dynamics of the atmosphere as well as a structural change. It is likely that above the transition, vertical eddy transport is no longer as effective in supporting the haze and we see a vertical haze distribution closer to the natural fallout time. Hapke (1975) sees correlation of bright clouds with polarization, indicating that at least the tops of the UV markings must reach near 70 km, since multiple scattering at 65 km and below would destroy polarization effects.

One result of the observations so far discussed is that it is possible to put limits on what we see in the Mariner 10 UV images. The evidence points to variable atmospheric activity on both large and small scales within the limits h = 65 $\pm$ 5 km, P = 150 $\pm$ 100 mb, T = 250 $\pm$ 10°K. Whatever motions we

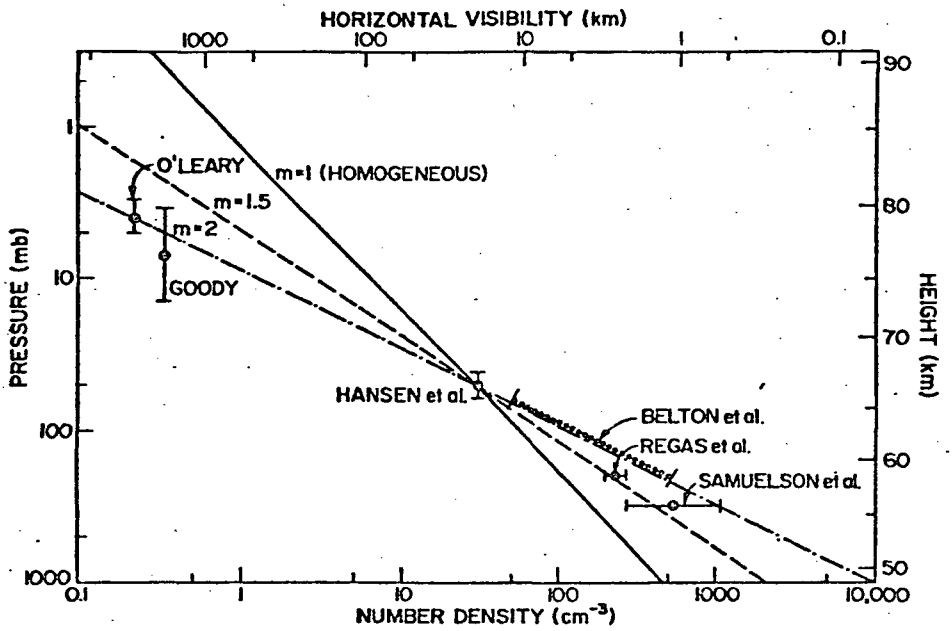

Figure 2. Cloud particle distribution in the upper atmosphere of Venus (from Lacis, 1975). The number m is the ratio of gas scale height to particle scale height. The data points are for measurements of various types: limb haze and star transit on the left, polarization in the center, and CO_2 absorption on the right. The number density and horizontal visibility scales assume 1.05 μm particles and m = 1 and should be linearly scaled for other values of m. The ratio of scale heights shows a tendency to change around 50 mb. Assuming the gas scale height is constant, the particle scale height is about 50% less above 70 km.

measure must lie primarily within these limits, and whatever structure we see is probably correlated with dynamical processes on Venus and limited to vary within the narrow limits just mentioned. It is highly unlikely that all visible phenomena in a 10 km thick slice of atmosphere will be decoupled. Determining what the clouds really are, and what mechanisms affect their form and evolution may be difficult, however,

The lapse rate between 60 and 70 km altitude is no greater than 3°K/km (Marov, 1972, Howard, et.al., 1974), which is strongly sub-adiabatic and would tend to inhibit convection and vertical mixing. The size of the convective cells seen by Murray, et.al. (1974) (~200 km) compared with the vertical structure observed (3-4 km scale height, ~10 km visible thickness) tends to support widespread and somewhat shallow solar heating as a more reasonable explanation for the convection than localized release of latent heat. The >20:1 ratio of width to height is also more representative of Benard cells than convective storm towers on Earth. Murray, et.al. (1974) ascribe the quickly varying temporal behavior of the markings to a condensate rather than to dust, but can reach no conclusion as to whether the clouds are bright features in a dark absorbing medium, or dark features in a bright scattering medium. A serous problem is that no suitable condensate has ever been proposed for the clouds of Venus which could fit all the evidence.

Even sulfuric acid droplets, once formed, may change size or H_2O content a few percent, depending on local heating or vapor pressure but will not completely evaporate again unless subjected to much higher temperatures (Young, 1975, Prinn, 1975). Such droplets can exist in equilibrium with little physical change over a range of two orders of magnitude in water vapor concentration and over a wide range of altitudes and temperatures on Venus. The cloud haze on Venus forms small scale features and dissipates them as well over times as short as a few hours. Thus, the UV markings are as unlikely to consist simply of evaporating acid aerosol as they are to consist of dust.

The stable lapse rate virtually guarantees the presence of waves between 60 and 70 km. At the very least one can predict a solar thermal tide. The subsolar convection zone is a possible mechanism to excite such waves. Therefore, the question should not be whether there are waves on Venus, but what kind? What are the dominant modes of oscillation and how are they excited and coupled to each other? Murray, et.al. (1974) report: (a) bowlike waves - moving at a slightly slower speed than the mean zonal equatorial flow and intensifying as they move toward the evening terminator; (b) circumequatorial belts - drifting across the equator from north to south; (c) Y features - appearing to be formed in part by the spiral streak patterns and having a 4 day periodicity. Belton, et.al. (1976) have found that the intensity of the Y feature is also modulated with a 4 day period. In light of the observed differential zonal motion of the small scale features, they conclude that the contrast variation is wave related since it moves with the 4 day equatorial features but against the faster mid latitude features.

One can observe in Figure 1 that the polar ring oscillates in latitude. There could therefore be a meridional motion oscillation related to the Y feature and its intensity variation. The variable CO_2 concentration hints at vertical oscillations on a large scale, while the wide spread of measured zonal velocities hints at variations in the zonal flow. It may be impossible

to determine the "mean" state without a continuous series of observations over a long time. This must be kept in mind in interpreting any results from a limited series of Mariner 10 images, although we can say that the appearance of Venus during the flyby would seem to be its most usual appearance.

The fact that a number of wavelike phenomena are visible at all in the UV images is remarkable. Surely, as we have indicated, one ought to expect waves. One should not, however, given the appalling lack of reasonable condensates, expect to see all of these waves. The fact that we see so much wavelike detail indicates that the UV absorber is modulated by very subtle changes in the balance of pressure, temperature, and altitude within the previously stated limits ($T = 250 \pm 10°K$, $h = 65 \pm 5$ km, $P = 150 \pm 100$ mb). It is hard to ascribe this to anything but a phase change. Sulfuric acid freezes within these limits, and it is possible that scattering off the solid aerosol surface could modify the effect of UV absorption inside the droplets or in the surrounding medium. The presence of HCl and HF as impurities in the H_2O - H_2SO_4 system makes the physical chemistry very difficult to specify, however, and too corrosive to do exacting laboratory tests needed to determine phase diagrams.

It is apparent that while there are numerous established facts, there is as yet no clear interpretation of them. What must be kept in mind is that regardless of what the clouds of Venus consist of, or what color they are, or what causes them to evolve the way they do, we can confidently say that they move in a certain way on a global scale. The implications which derive from such motions are significant for understanding the general circulation of Venus, for they will permit us to separate wavelike motions from mass motions, to understand the physical scales at which dynamical phenomena of a given type are occurring, and to bound the range of dynamic models which can explain the general circulation.

II. IMAGE GEOMETRY AND NAVIGATION

The Space Science and Engineering Center at the University of Wisconsin has a large number of Experimenter Data Record (EDR) tapes copied from the original set at the Jet Propulsion Lab. These raw image tapes will form the bulk of our future wind analysis program. To minimize the amount of preparation and programming time necessary to use the image data, a small subset of 18 images of Venus was preprocessed at the Image Processing Laboratory (IPL) at Jet Propulsion Lab using the well known programs FICOR and GEOM, originally developed for the Mariner 9 Mars Orbiter mission and adapted for Mariner 10 (Soha, et.al., 1975). Relative photometry of a few percent and geometric accuracy of ~1 pixel is obtainable throughout most of a TV frame. The pictures were photometrically decalibrated, and then geometrically rectified (remapped to object space) with a scale factor such that the planet disk is the same apparent diameter in each picture and free of gross distortions.

Two time lapse sequences were generated from the decalibrated images, one with 25 km/pixel ground (cloud) resolution, and the other with 15 km/pixel resolution. The higher resolution sequence, containing 4 images spanning a 3 1/2 hour time period, was chosen to provide the initial cloud velocity profile. The lower resolution pictures form a longer time sequence covering 16 hours. This series more clearly shows the large scale UV markings and bowlike waves, but has not yet been extensively analyzed. We intend to eventually measure several sets of full disk images to improve statistics and determine if there are measureable changes in the global velocity distribution from day to day.

A. The Man-computer Interactive Data Access System (McIDAS)

The image alignment, time lapse display, and motion measurement is done using the Man-computer Interactive Data Access System (McIDAS) developed at the University of Wisconsin Space Science and Engineering Center.

McIDAS is designed to optimize the mixture of analog processes, digital processes, and human processes used in image analysis. The system is designed around a Datacraft 6024/5 mini-computer control system with 24 bit 64 K word memory. The computer has four basic functions:

1. Control of bulk data input/output processes (analog and digital)
2. Computational tasks
3. Control and coordination of a video display system
4. Interactive communication and response in real-time with scientists, graduate students, or operations personnel.

The basic operational approach for the McIDAS system has the operator in front of a color TV monitor. He has a keyboard and a joystick, which allows him to interact simply and effectively with the computer in a mechanical and verbal command "language". With these controls, the operator tells the computer the type of data to display, the scale and format he wants to see, and

the type of enhancement and image blending or pixel interlace he wants to use. The computer translates his requests into specific commands and sequences of commands which are transmitted to the peripheral display system hardware, which in turn presents the requested display to a color monitor. The operator then examines the display, performs judgement, selection, or decision functions, and directs the computer to perform measurement or analysis functions on the specific data sample selected. The computer recovers the required data sample from the original digital data in the archive, processes the data to the condition selected by the operator, performs the measurement or analysis function and presents the results. Usually the results will be in the form of another display on the color monitor, or a few lines of printout on a CRT display. The entire set-up is geared to let McIDAS do the data transfer, editing, and quantitative manipulations while the operator provides the selection and judgement functions.

The Mariner 10 images, photometrically and geometrically decalibrated to maximum possible precision, are thus input to a measurement and display system which allows none of the original image precision to be lost in measurement, yet permits highly complicated interaction of a guiding scientist with both the data and the data processing in near real-time. Most display systems lack intelligence and precision. Most measuring systems lack intelligence and speed. McIDAS combines speed, precision, and the operator's intelligence in a truly "interactive" system, using an optimized combination of analog, digital, and human capabilities.

B. Image Navigation

The motion of the clouds on Venus is measured in the Mariner 10 TV images in image coordinates. To get velocities, the motion must be determined in a Venus reference system. Thus, we need to define a transform which converts from line-element or pixel coordinates to latitude-longitude or Venus coordinates. We call the definition and use of this transform "Image Navigation". Once done properly, it is possible to tell where on the planet each pixel in the TV image lies, or inversely, which pixel corresponds to a given latitude and longitude.

Two approaches can be used. The first approach is to apply the navigation transform directly to the image data before measuring cloud motions. Computer programs have been developed at JPL which map a geometrically rectified TV image into any number of standard cartographic projections. These have been used to produce maps of the moon, Mars, and now Mercury. The programs require input from the Supplementary Experimenter Data Record (SEDR) which converts engineering data on spacecraft attitude, spacecraft mass distribution, drift rates, trajectory position, scan platform backlash, camera mounting angles, etc. into a best estimate of where the TV camera optic axis intersects the planet. This information is useful as a first estimate, but the error in determining absolute pointing angles from engineering data (0.1°) would have been larger than many of the cloud displacements we were attempting to measure.

IMAGE NAVIGATION

a) BEST FIT TO A SPHERE:

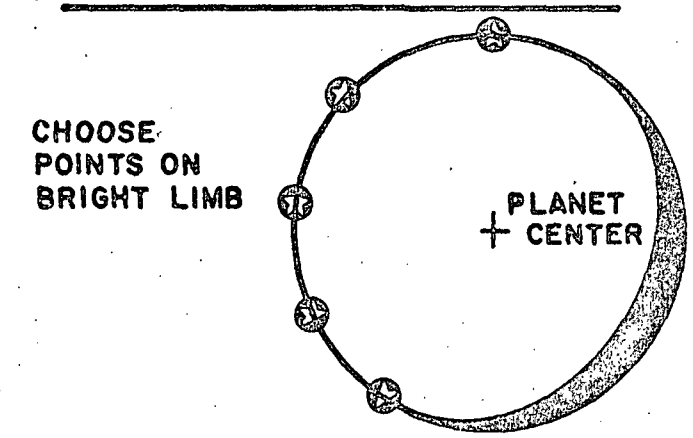

b) PLANET GRID DEFINITION:

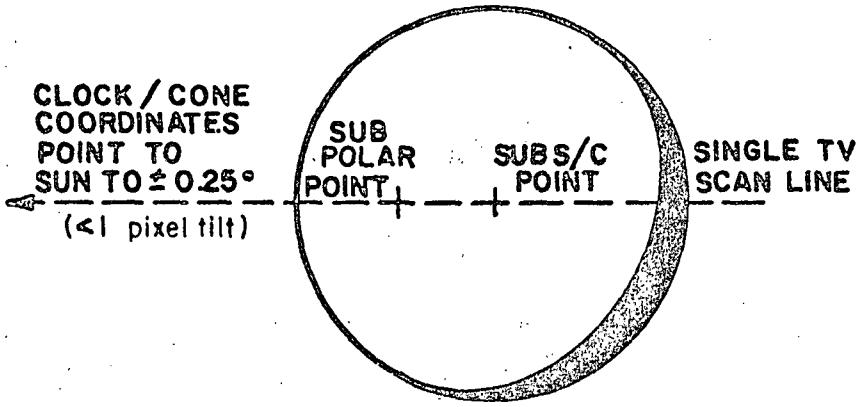

INPUTS

- LIMB POINT COORDINATES
- LINES PER FRAME
- ELEMENTS PER FRAME
- HEIGHT OF FRAME (deg)
- WIDTH OF FRAME (deg)
- DISTANCE TO VENUS SURFACE

- LATITUDE OF S/C SUB POINT
- LONGITUDE OF S/C SUB POINT
- LATITUDE OF SUB SOLAR POINT
- LONGITUDE OF SUB SOLAR POINT

Figure 3. Image navigation occurs in two parts. Part (a) shows the best fit to a sphere using the image data, viewing geometry, and camera calibration. This determines the scale of the planet navigation model. Part (b) shows how the epoch and trajectory information from Mariner 10 is used to place a latitude-longitude grid on the navigation model with the proper orientation.

The second approach is to make measurements of cloud displacements in TV image coordinates and then apply the navigation transform derived from the images themselves to the displacement vector. Provided the spacecraft is far enough from the planet to see the bright limb, there is enough information in the original images to uniquely determine camera pointing angles with respect to Venus. The use of the images themselves theoretically permits determining camera pointing angles to the order of a pixel (9.4 μr) rather than 0.1 degrees. We chose, therefore, to initially measure cloud motions in images where a substantial portion of bright limb was visible (~150 degrees of arc).

The navigation model used consists of two parts (Figure 3a and b). Part one is the best fit to a sphere. Five to ten points are chosen at a DN threshold on the bright limb and a least squares fit is made to determine the center of the planet. The residuals of the five points must be within one resolution element (pixel) of the assigned radius of the planet plus cloud deck. Using data supplied by O'Leary (private communication) we chose to define the limb radius at 6131 km for a brightness threshold of 35-40 DN. This is approximately the $\tau = 1$ slant optical depth for the UV images.

The value of the radius is not crucial since it only affects the scale of the navigation model. Provided we stay away from the limb when measuring (to avoid foreshortening) an error of 60 km in assigned radius would be only a 1% error in the scale of the displacement vectors (~1 m/s). What is very important, however, is that the radius and brightness threshold be consistently chosen, for if the planet centers are inconsistently found, the absolute displacement error from one frame to the next transfers directly to the measured cloud displacements. For example, a 60 km error in determining or aligning planet centers in successive frames could yield a 16 m/s velocity error over a one hour time interval between pictures.

The required inputs to obtain the best fit to a sphere are:

1. Coordinates of 5 limb points
2. Lines per TV frame
3. Elements per TV frame
4. Angular height of frame
5. Angular width of frame
6. Distance to Venus surface (altitude)

The angular size of the TV frame is accurately known from camera calibration. The black mask framing the vidicon and the focal length of the telescope precisely define these parameters. The angular distance between reseau marks is also well known from the camera calibration. Thus, by choosing reseau pairs and measuring the distance between them in lines or elements, one can determine the lines and elements per frame as well as the magnification factor applied during the geometric decalibration. Calculation of the aspect ratio (element to line ratio between reseaus) allows a double check on the consistency of the measurements. The altitude of the spacecraft is well known from trajectory data. Table I shows the results of the image geometry determination.

The next step is to verify that using the geometrically decalibrated and scaled images, we can get the navigation models to properly align with each

TABLE I

IMAGE GEOMETRY

From Resau Measurements
on Rectified Venus Frames

MVM '73 A CAMERA: FOCAL LENGTH 1495.66 mm

FRAME HEIGHT 0.3663 deg

FRAME WIDTH 0.4723 deg

FDS	SHUTTER TIME GMT		# RESEAU PAIRS MEASURED HORIZ.	VERT.	MEAS. FRAME SIZE LINES	ELEMENTS	ASPECT RATIO	MAG. FACTOR
62693	039	020656	12	9	799.932	965.366	1.206	1.099
62839	039	034908	6	7	824.386	993.344	1.205	1.132
62857	039	040144	11	9	828.075	997.616	1.205	1.137
62987	039	053244	12	9	849.175	1024.543	1.206	1.167

TABLE II

IMAGE NAVIGATION

(For 5 Point Fit)

MVM '73 A FRAME: .3663 x .4723 deg.

35-40 DN THRESHOLD AT 6131 km

FDS	HEIGHT (km)	FRAME SIZE FROM RESEAUS LINES	FRAME SIZE FROM RESEAUS ELEMENTS	BEST FIT FRAME SIZE (NAVIGATION MODEL) LINES	BEST FIT FRAME SIZE (NAVIGATION MODEL) ELEMENTS	RMS RESIDUALS AT LIMB (km)	NAVIGATION MODEL PLANET CENTER LINES	NAVIGATION MODEL PLANET CENTER ELEMENTS
62693	1694932	800	965	802	968	14	447	597
62839	1745295	824	993	828	994	0	447	596
62857	1751505	828	998	830	998	11	446	597
62987	1796354	849	1025	849	1024	5	447	597

GROUND RESOLUTION ~15 km/PIXEL AT

SPACECRAFT SUB POINT

other from image to image. Table II shows those results. The frame size of FDS 62693 required a change of 2-3 pixels (with the angular size fixed) to obtain the best fit, indicating that either the altitude or chosen magnification factor for remapping the image was probably incorrect by 0.2 - 0.3% for that frame. However, since we are directly using the image data to navigate, no scale factor error is introduced. The planet centers and limbs all agree and align with each other to 1 pixel or less.

The second part of the navigation procedure, once one has obtained the best fit to a sphere, is to put the latitude longitude grid on the planet. The basic inputs are:

1. Latitude of sub-spacecraft point
2. Longitude of sub-spacecraft point
3. Latitude of subsolar point
4. Longitude of subsolar point

The sub-spacecraft point is known extremely well from trajectory data which had to be reduced early in order to make course corrections to get to Mercury. This point is identical with the planet center in the images. The latitude and longitude of the subsolar point is also well known from celestial mechanics and radar. The 3 axis stabilized spacecraft was held to its attitude within a limit cycle of ± 0.25 degree in each axis. Since the camera was mounted on the scan platform in a clock-cone coordinate system, every scan line in the TV image points to the sun to approximately ± 0.25 degree, and the subsolar point and sub-spacecraft point must therefore both lie on a single scan line. With the best fit to a sphere defining the planet scale, and with the sub-spacecraft point used as an anchor point; the latitude-longitude grid is rotated until the given subsolar point lies on the same scan line as the planet center. This completes the definition of the navigation geometry.

The maximum deviations from picture to picture in pitch, yaw, and roll (determined from the Mariner 10 engineering data tapes) were: pitch, 0.108°; yaw, 0.237°; and roll 0.144°. Thus, the maximum scan line tilt of the camera between any picture pair is less than 0.3°. A 0.3° tilt of a scan line corresponds to <1 pixel error in attitude for subsolar and sub-spacecraft points ~175 pixels apart. There is also ~1/2 pixel error in roundoff and truncation possible in the navigation model because integer pixel coordinates are used. As a result, the total RMS error in navigation (including image rectification) is ~2 pixels (Table III). As we shall see later, the correlation methods used in measuring cloud displacement interpolate to better than 0.1 pixel, so measurement error by the computer is negligible. When the McIDAS operator uses single point tracking so that he measures the displacement himself by positioning the cursor on a point, one has to increase the RMS error. There is a 1 pixel granularity in cursor position plus up to several pixels for operator accuracy, so the anticipated RMS error for operator measured cloud displacements is 4-5 pixels. That is about double the error for the computer measurements, where the operator merely selects a cloud target with the computer doing the measuring. As a result, we must treat single point tracking measurements separately in the motion analysis since they can be expected to have larger scatter.

TABLE III

ERROR SOURCES

GEOMETRIC RECTIFICATION	~1 pixel
NAVIGATION MODEL FIT	~1 pixel
LAT-LON GRID DEFINITION	~1 pixel
ROUNDOFF & TRUNCATION	~1/2 pixel
RMS ERROR	~2 pixels

SP TRACKING ADDS 1 PIXEL GRANULARITY IN MEASURING PLUS UP TO SEVERAL PIXELS FOR OPERATOR ACCURACY, THUS THE RMS ERROR IS ~4-5 PIXELS

TABLE IV

VELOCITY ERROR

(15 km/pixel Resolution)

PIXELS SHIFTED	km SHIFT	VELOCITY INCREMENT FOR A GIVEN TIME INTERVAL(m/s) 15 MIN.	30 MIN.	1 HR.	1-1/2 HR.	3 HR.
1	15 km	16 m/s	8 m/s	4 m/s	3 m/s	1.5 m/s
2	30	32	16	8	6	3
4	60	67	33	16	10	5
6	90	100	50	25	18	9

Knowing the expected errors in alignment and measuring, we can predict the velocity errors we should expect. Table IV shows the situation for the 15 km/pixel resolution data. For a 2 pixel error, any time interval greater than 1 hour between frames will give <10 m/s uncertainty in the measurements. For a 4 pixel error, we need a time interval over 1-1/2 hours to do as well. For 5 m/s accuracy, we need time intervals of 2-3 hours at this resolution.

One pair of frames (Table I) had a 13 minute time interval. True to expectations, we found scatter in the measurement as high as 70-80 m/s, so this short time interval, T_2-T_3, was not used for velocity determinations. Five other time intervals formed from the four 15 km/pixel resolution images were found acceptable: T_1-T_2, T_1-T_3, T_1-T_4, T_2-T_4, T_3-T_4. These time intervals formed the basis for the initial measurement of the global velocity field on Venus reported here.

III. CLOUD MOTION MEASUREMENT

In addition to image navigation, it is important to understand the measuring process in order to judge the significance of the results. The entire 8 days of Mariner images of Venus exhibit characteristics similar to the most common ground based observations, e.g. the 4-day rotation, reversed "C" features, "Y" features, and two bright polar rings or caps. It is reasonable, therefore, to assume that the Mariner 10 observations are representative of Venus as it usually is. If the meridional motion and the zonal motion, as measured, are both representative of the mean state of the upper atmosphere, it then becomes possible to set some boundary conditions on the general circulation.

A very important consideration to keep in mind is the confidence one can place in deviations from the velocity structure we see. Provided one believes in the accuracy of the navigation and the measurements, the scatter in the u-component is significantly larger than it should be. We also observe a small number of deviant measurements, again significantly more deviant than should be expected. This has made us look more closely at the possibilities of additional structure superimposed on the vortex and at vertical shear and varied kinds of wave perturbations on the steady state. Evidence for these phenomena can be found in the images, but the best quantitative measures we have to date rest in the "significant deviations" mentioned above. Study of such second order effects in the data may be a major part of future analysis.

A. Motion Measurement Techniques

Large scale features can be easily traced across the full disk of Venus, but smaller features <200 km across are harder to track. They have low contrast, they may appear and disappear either by changing shape or brightness substantially so as to become unrecognizable over periods of a few hours, or they may just fade away into a background of pulsating light and dark features. It should be noted here that by pulsating brightness, we are talking about relative contrast variations of a percent or two. The images must be contrast stretched to a high degree to see anything at all, and it is not unreasonable to expect that some of the variation is due to quantization roundoff in the cameras. In general, one can say that the longer the time interval, the harder it is to follow a feature. The shorter the time interval of observation, however, the less accurate the velocity determination. We initially tried several techniques to ascertain the differences between them and their relative accuracies on the same or similar cloud targets.

Measurement of cloud motions is done in the TV images of Venus in two ways. The first method is called "single point tracking." The McIDAS operator, using a joystick, superimposes a cross cursor on the TV screen over the Venus image played back from a track on an analog disk. Since the cursor is electronically generated on the TV screen, there is no parallax. The operator chooses a cloud feature, moves the cursor to coincide with the feature, and presses a key on his communication console. The computer inquires of the cursor electronics where the cursor is positioned in the TV image relative to the analog disk timing track and receives a line-element image coordinate accurate to ~1/2 pixel.

The analog disk head is advanced automatically to the next TV frame in the time sequence being analyzed and the operator moves the cursor to the new position of the cloud he is tracking and again presses the key. The computer records the second set of coordinates and calculates a displacement from the first position in lines per hour and elements per hour. The Venus navigation model can then be applied to transform the vector magnitude and direction to planet centered U and V components and meters per second.

The second method of measuring motions utilizes the computer to do objective image matching rather than the operator. The operator chooses a cursor size and shape in the form of a k by ℓ pixel box. The cursor box is then positioned over a cloud or cloud feature to define an image target grid A (Figure 4). A lag size s is defined such that when the operator pushes the key on his console the digital data in image grid A is moved from digital disk to core, and the cursor is enlarged to a m by n box where $m = k + s$ and $n = \ell + s$. The frame is advanced and the operator places the enlarged cursor over the same cloud target at the new time and position and then presses the key to define the image search grid B. The grids A and B are then compared over all the different possible lag positions (p, q) and a match coefficient matrix generated (Fig. 4b, 4c, 4d).

The image match coefficients are constructed as vector products using varied norms. The Cross Correlation Norm (CC) is simply a direct product of the elements in A and B, the "angle" between the two "vectors". The Euclidean Norm (EN) is the "distance" between the grid vectors, the square root of the sum of the squares of the products. Any LP Norm can be generated as well. The difference between the norms is that the lower power norms are more sensitive to edges and image details. The higher power norms are more sensitive to light and dark patches. The Euclidean Norm seems to be more sensitive to image detail in general, emphasizing neither edges nor area contrast. Because the target clouds varied in structure and were diffuse and changeable with time, we chose to measure each target with single point tracking (SP) and the norms CC, EN, and LP5. We expected to find differences between edge and patch tracking because of the observed variability of the clouds with position on the planet.

At each lag position the match coefficient matrix is searched to find the particular lag position at which the best match occurs (usually the greatest relative maximum). The lag position corresponds to the displacement of the cloud in grid A over the T_1-T_2 interval. The peak of the image match

Figure 4. (a) Computer image matching is done by moving the data in Target grid A around in Search grid B until maximum correlation is achieved.

(b) Image match coefficient matrix for an image correlated against itself, a perfect match.

(c) Image match coefficient matrix for a good correlation in the Venus images.

(d) Image match coefficient matrix for a correlation failure. Note the broader peak and lack of a well defined maximum within the matrix boundaries.

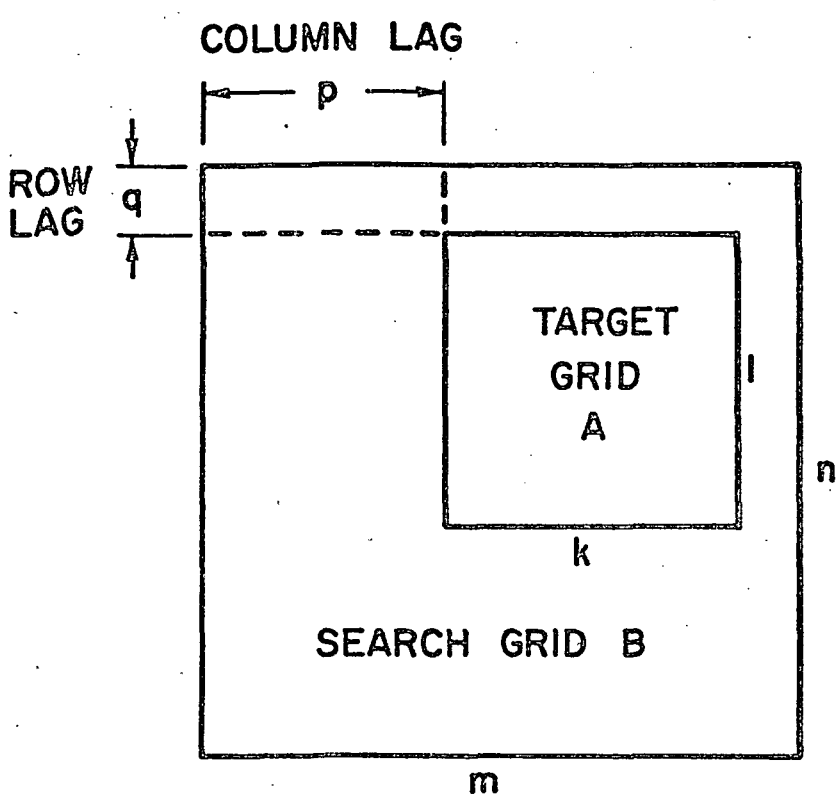

(a)

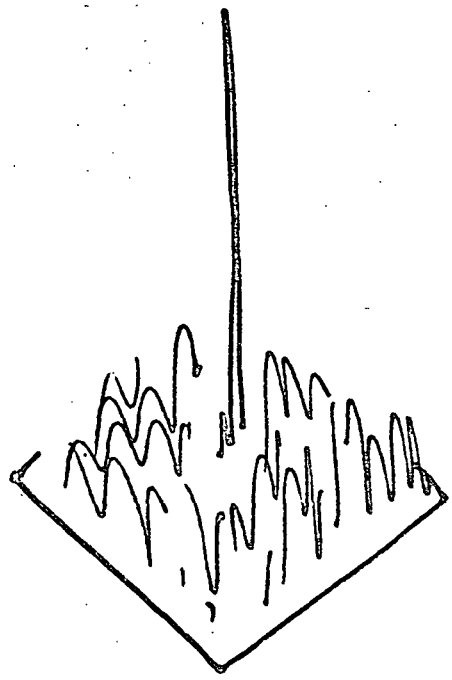

(b)

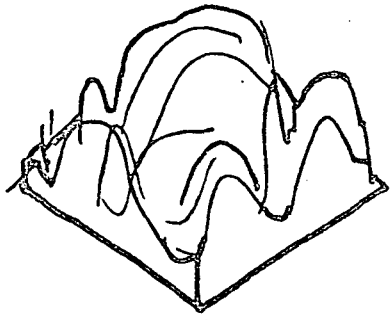

(c)

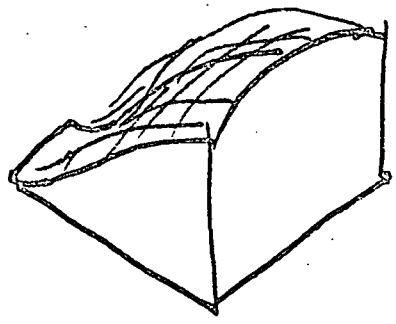

(d)

FIGURE 4

coefficient matrix represents the best match of the target grid with the search grid. The difference between the (0,0) lag coefficient coordinate and the best match coefficient coordinate is determined by quadratic interpolation in 2 dimensions in the image match coefficient matrix. The cloud motion displacement vector is determined in image coordinates. Transforming the lag displacement vector end points to Venus coordinates results in the wind estimate.

Because of the cofficient matrix interpolation there is no granularity in the computer displacement measurements as there is in single point tracking by the operator. With Earth clouds, we have determined the interpolation to be accurate to <0.1 pixel. The Venus cloud data is much more diffuse and less contrasty, however, with a significant lack of detail. As a result, many of the correlation peaks, especially away from the Venus equator, were quite broad. If the correlation surfaces or image match coefficient matrices did not have a well defined relative maximum, they were rejected by the computer as correlation failures.

The failures were in large part due to the fact that a cloud feature had evolved so much as to become unrecognizeable to the computer. In most cases, single point tracking was still possible since the operator has the advantage of seeing coherence of the feature in time and can move forward and backward in the multi-picture loop until he has the target clearly recognized. The computer only has two image grids to compare and can utilize no other information. The computer is more precise, but inherently subject to more confusion. This points out the need for consistency checks on the computer measurements. If the same velocity is not measured over successive time intervals for the same cloud target, the computer may have lost the target or latched on to a nearby cloud which was similarly shaped. A target giving vastly different velocities when measured over different time intervals and with different norms must be suspect as not passive enough to be a good wind tracer and must be rejected. Unfortunately, the scatter in individual measurements in the Venus data was too great to use such a quality control criterion. A statistical approach to analysis was used instead.

B. Velocity Measurements on the Mariner 10 Venus Images

Targets were chosen in the four 15 km/pixel images on the basis of their discriminability and ease of tracking. The cloud features were generally of too low contrast to be clearly discernable in the raw images. Most of the time the image on the McIDAS TV screen had to be contrast enhanced or occasionally even high pass filtered to aid discrimination of features by the operator. Thus, SP tracking could possibly be biased by artifacts introduced in the enhancement or filtering process. To provide a control on such a possibility, the computer is required to do correlation and image matching only on the "raw" unenhanced data for the EN, CC and LP5 norms. "Raw" data has only been subject to noise spike removal, photometric correction for removal of vidicon shading, and geometric rectification for removal of distortion in the camera deflection system. Such images are as close to the true scene information as possible and free of processing artifacts introduced by computer filtering. Thus, different measurement techniques operating in parallel can be used as a trap

to catch biases or as an indicator of subtle differences in cloud characteristics not readily apparent to the operator.

SP tracking involves only the designation of a line element coordinate for each target. There is no image matching surface to examine. The acceptance rate for such measurements is therefore 100%. The "objective" computer tracking algorithms were applied by placing the center of the joystick operated cursor at the center of the cloud target, making the rectangular cursor box large enough to contain the target. All 6 image pair combinations were tried with each of the four norms. With the 3 computer norms, however, the computer had to examine each resulting image match surface to find a well defined maximum correlation peak within the bounds of the surface. No peak, or a maximum at the outer edge of the surface caused the computer to label the correlation a failure. More than 20-25% failures on a target would indicate that the computer was having difficulty. In such cases, the target was rejected by the operator and a new target chosen for measurement. A final measurement set of 47 targets and 1067 vectors was produced.

It is instructive to examine characteristics of the target tracking techniques in operation. Some cloud targets change substantially in size and shape over the longer time intervals of 2-3 hours. As a result, more operator indecision over the exact position of the target was noted, and the computer had a lower success rate in making image comparisons in the raw data. On the other hand, there was no difficulty encountered following features in the 13 minute time interval for either the operator or the computer, but the velocity measurement errors were proportionately larger. The short time interval was found especially useful in identifying vertical wind shear, but did not provide very accurate measurements.

We conclude that the optimum observation appears to be 15-20 minute time resolution over a time interval of at least 4 hours, a sequence of roughly 10 time lapse images. The high time resolution provides continuity for tracking purposes while the longer time interval provides greater accuracy in the velocity measurements. The lack of observed cloud features on Venus at resolution better than 10 km would seem to eliminate the need for higher time and space resolution. If one has poorer ground resolution than 15 km, the time intervals become proportionately larger, and the ability to resolve small velocity increments is reduced. These facts should be kept in mind when designing an optimum imaging system to study atmospheric dynamics from the next generation Venus orbiters.

The performance of the three computer cloud tracking techniques surprisingly yielded no discernable differences in accuracy. If a correlation was possible, the EN, CC, and LP5 determined velocities averaged out with nearly the same target means and the same amount of scatter to within 1-2 m/s. Given velocity profiles determined by the three different techniques, it would be impossible to distinguish which velocity profile was made with which technique. For that reason, we will treat all the computer measured volocities (EN + CC + LP5) as a single data set, designated by COMP.

While the velocity measurements were similar, the target tracking abilities of the three computer norms were not the same. As expected, the LP5 norm was more successful in the patchy sub-solar region. The streaky clouds in the mid latitudes were difficult for LP5 because the light and the dark patches were

too large and too diffuse to provide a sharp correlation peak. The useful image information in mid latitudes resided in the edges of features, so the CC norm was more successful there. The EN norm was useful almost everywhere and seems the best compromise technique given the varied structure of clouds on Venus.

The best success in target tracking on Venus was obtained by staying away from the limb to avoid foreshortening, and by staying at least 40 degrees in phase angle away from the terminator. As one moves closer to the terminator in the images, the first noticeable effect is a loss of contrast. Features are harder to follow because as the scene brightness diminishes, the digitization level for any intensity becomes a larger fraction of the scene dynamic range. The net effect is to lose both spatial and photometric resolution as neighboring pixels are quantized into the same gray level in the camera, producing a very contoured image. Near the terminator itself, no cloud detail is apparent, only contours of uniform gray. Generally, if the McIDAS operator would follow a cloud feature easily in the enhanced or filtered image, the computer could track it in the raw image. Where the operator had trouble, so did the computer. A practical limit of 230° longitude was established to define the bound of the "difficult" tracking region on the planet. Figure 9 shows this region to include about 40% of the visible disk of Venus.

A loss of 40% of the observable area of the planet is substantial. We plan to pursue cloud motions in that region in some fashion, possibly in higher resolution images, since the velocities in the morning terminator part of the planet could have bearing on definition of the drive mechanism for the zonal winds.

The bias catching trap, mentioned earlier, did catch something during the analysis which is of significant value. While the v-component (meridional) averages of SP, EN, CC and LP5 show no significant differences, the u-component (zonal) velocities determined by SP consistently average 5-10 m/s larger than the computer determined velocities. Moreover, the RMS scatter in the measured u-component is 2-3 times the RMS scatter in the v-component for all four norms. One place to look for an explanation is in the image navigation, and another is the McIDAS operation. Those possibilities are examined next.

C. Vector Data Set Selection

The vectors generated from the 13 minute time interval between the second and the third pictures in the sequence had unacceptably large scatter in the measurements, with some vectors ranging as high as 60-70 m/s from a target mean, which generally was determined from an average of about 15 computer measurements (6 for the SP target means). From Table IV this result is expected. Consequently only the 5 longest time intervals were used, reducing the sample to 887 vectors. The individual target means were then recalculated on the basis of the remaining 5 time intervals.

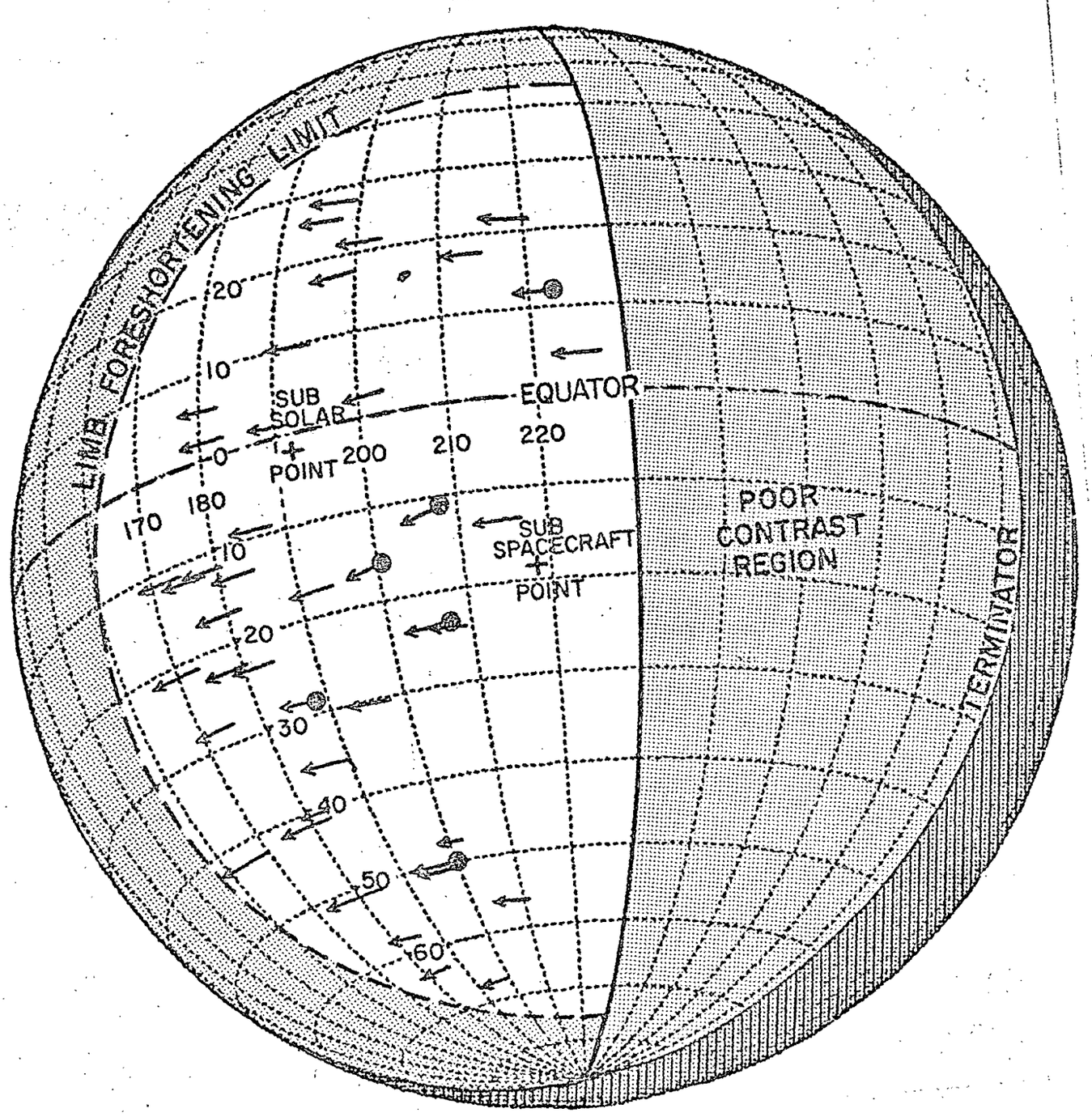

Figure 5. Appearance of Venus in the measured images 2 1/2 days after encounter. Crosshatched portion is the portion not illuminated by the sun. Shaded areas are regions containing no measurements due to poor contrast or foreshortening. Each arrow represents one cloud target, with the solid dots identifying the location of the six "wierd" targets. Note the bias introduced by the fact that cloud targets above 30 degrees latitude lie at the leftmost longitudes.

TABLE V

Mean Measured Velocities and RMS Deviations

	NORM	NUMBER OF VECTORS	u		v	
			MEAN OF ALL VECTORS	RMS DEV. FROM TARGET MEANS	MEAN OF ALL VECTORS	RMS DEV. FROM TARGET MEANS
46 TARGETS 5 TIME INTERVALS	SP	381	-103.89	16.55	-3.75	6.60
	COMP	506	- 91.20	14.00	-1.53	8.54
15 m/s CUTOFF	SP	256	-101.14	7.37	-3.40	4.72
	COMP	364	- 91.36	5.93	-0.06	4.96

TABLE VI

Velocity Correction from Image Misalignment Test
(All vectors, SP and COMP)

IMAGE PAIR	TIME INTERVAL	VELOCITY CORRECTION (RMS)		
		2 Pixel Estimate from Table IV	Actual Δu	Actual Δv
T_1-T_2	102 min	4.9 m/s	1.72 m/s	.44 m/s
T_2-T_3	13 min	32.0 m/s	22.4	1.62
T_3-T_4	91 min	5.5 m/s	1.56	.39
T_1-T_3	115 min	4.4 m/s	3.85	.41
T_1-T_4	206 min	2.4 m/s	1.99	.32
T_2-T_4	104 min	4.8 m/s	1.52	.26

TABLE VII

Summary of Cloud Motion Vector Selection

	VECTORS REMAINING
Initial Data Set (47 targets)	1007
13 Minute Time Interval Rejected	887
15 m/s Edit to Sharpen Distributions	620

A large RMS scatter still remained in the measurements (Table V). It was decided to discard about 1/3 of the most deviant measurements to sharpen the distribution. Care had to be taken to avoid throwing away any maxima and minima in the velocities as functions of latitude or longitude. We could not simply calculate an average over all latitudes and longitudes and throw away the fastest and slowest vectors. Instead, the mean velocity in u and v for each separate cloud target was used, so that the deviation of a vector from its own target mean was the criterion for rejection. Provided targets were not substantially accelerating, such a selection technique would preseve latitudinal and longitudinal structure of the cloud motion field, as well as isolate targets with motion anomalously different from the majority. The 6 "slow" targets seen in the COMP measurements are anomalously different in this sense. They are therefore deserving of more study.

The fact that the scatter in the u component is 2-3 times the scatter in v requires explanation. This cannot be explained in terms of a systematic bias in the measuring process because of the matrix transforms and planet tilt, which linearly combine x and y image directions in nearly equal proportions to generate u and v. A single McIDAS operator (Krauss) made all target selections and measurements. The use of a single person to make the measurements was advantageous from the standpoint of consistency, but introduces a greater risk of bias. Any tracking bias would, however, have to occur before the matrix transform from line-element to latitude-longitude coordinates. We feel that it would be impossible to intuitively grasp the necessary time and geometry relations necessary to bias over 1000 measurements made with vastly different techniques over a variety of surface orientations in different places on Venus and still obtain consistent velocity profile patterns independent of time interval or tracking method. Thus, neither the different scatter in u & v nor the velocity profile shape seem related to operator bias.

Next, we examined the navigation procedure more carefully, looking for an underestimate of image misalignment, roundoff, or truncation errors. Each of the remaining 5 time intervals was separately examined. In each case the u component scatter was 2-3 times that in v. A program was written to take the average calculated latitude and longitude of the displacement vector in picture A, and use the navigation model for picture A to convert to line-element coordinates in picture A. The identical line-element coordinates in picture B were then taken and converted to latitude and longitude using the navigation model for picture B. This gave an independent quantitative estimate of image misalignment in terms of velocities instead of pixels. Table VI shows the RMS correction factors obtained, which are consistent with the v component scatter and the estimate in Table IV and nowhere near large enough to explain the u component scatter.

The Δu correction due to misalignment, roundoff, and truncation is around 1 pixel, slightly less that predicted. The v alignment is considerably better than expected. We do not know why! This correction is for systematic error in alignment, but random error in roundoff and truncation. Grid placement on the planet could vary by ~1 pixel between pictures and would impart a systematic rotation to the vectors. It is reasonable to say that we do

not fully understand what goes on at resolution below 1 pixel, but for this data set can still safely claim 5-10 m/s as our upper limit on systematic error in alignment and measuring, corresponding to ~2 pixels total misalignment and random error over the time intervals considered (see Table IV).

We conclude that the larger scatter in u is real and is probably due to actual time variations in cloud structure and vertical shear effects. The significant fact to keep in mind is that all evidence indicates measurement errors no larger than 5-10 m/s RMS while the "structure/shear" modifications are in the 10-20 m/s range. There is reason to believe, therefore, that second order effects in the cloud motions on Venus are measureable. We will return to this in the discussion in Section IV.

Cutoffs in u and v ranging from 5 m/s to 40 m/s from the individual target means were used to select vectors for plotting and least squares analysis. A 15 m/s cutoff was chosen as representative. Larger cutoffs left more scatter in the data, hiding its functional form, while smaller cutoffs threw away many more points without uncovering any added characteristics of the profiles. The 15 m/s cutoff threw out 30% of the most deviant measurements, leaving 620 vectors which formed our "cleanest" and hopefully unbiased data set. All analysis from here on is based on the 620 vector sample (Table VII).

IV. ANALYSIS OF CLOUD MOTION MEASUREMENTS

We present here the measurements of the motion of the small scale UV markings or cloud features. It should be possible now, in light of the previous discussion, to estimate the validity of the measurements and also to estimate the significance of the deviations and scatter in the measurements. We report in addition on observations of vertical wind shear and its organization. The facts are then summarized in Section V, and possibilities for further investigations using the Mariner 10 image data are examined.

A. Zonal Motions

Figure 6 shows the 15 m/s edited zonal velocities which were measured. Both SP and COMP velocities are shown, with the results presented both as separate target means, including RMS errors, and as scatter plots showing all 256 or 364 vectors, respectively, in the edited samples (see Table V and related discussions concerning vector selection). The SP measurements (Figures 6a and 6b) appear to have a 50 degree latitude velocity maximum. The COMP measurements (Figure 6c and 6d) are in better agreement with a maximum at 40 degrees latitude. Both SP and COMP data sets have approximately a -92 m/s minimum zonal velocity at the equator. A dashed line shows nearly constant angular momentum assuming -92 m/s equatorial zonal velocity and a linearly increasing decrement of angular momentum so the velocity at 45° is closer to 125 m/s than the 140 m/s if angular momentum were perfectly conserved. Least squares fits using second order polynomials were made to the measurements to determine a velocity minimum in the profile and assess the degree of symmetry about the equator. The polynomial fits were limited to latitudes less than 45 degrees. The results are presented in Table VIII and shown in Figure 6 as solid lines. At high latitudes, the measurements lie near a line of constant angular velocity, also shown dashed.

Figure 6c shows solid circles corresponding to the anomalous six "slow cloud targets" having lower velocities than their neighbors. They appear to be scattered randomly over the planet (See Figure 5) and are significantly different from neighboring cloud targets in that they do not show acceleration in the zonal direction (Figure 7c). The six targets lie close to a line of constant angular velocity, shown dotted in Figure 6c. The least squares fit between $\pm$ 45 degrees latitude without those slow targets is shown in Figures 6c and d as well as a separate least squares fit to the six slow targets. Visual inspection of the slow cloud targets in the TV images shows nothing distinctive about them with regard to shape, brightness, or position.

What is most surprising is that the low velocity cloud targets show up in the COMP measurements but not in the SP. This may be an example of how the precision of the computer measurements is affected by formation and dissipation at leading and trailing edges of clouds passing through a local pressure change or region of subsidence. The computer could thus be detecting an organized large scale wave phenomenon, as the constant angular velocity would seem to indicate. The McIDAS operator, tracking a center of brightness or

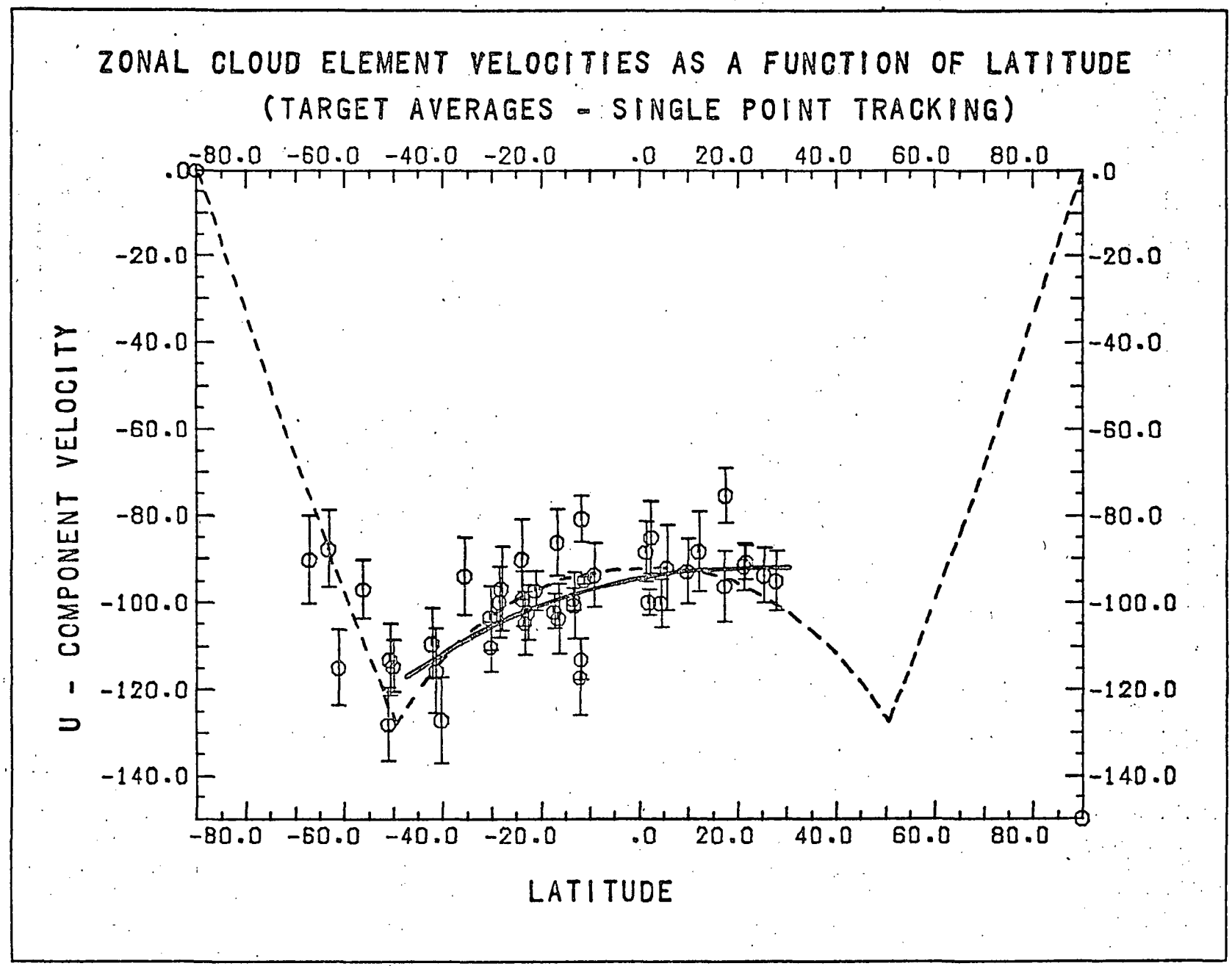

Figure 6a. Single Point Tracking using 15 m/s cutoff to edit data. Target averages are shown with RMS Errors. The dashed line is a model with a velocity maximum at 50° latitude, with nearly constant angular momentum at lower latitudes and constant angular velocity at higher latitudes, chosen to simulate a vortex as in Suomi, 1975. Solid line is least squares second order polynomial fit to data points within 45° of the equator.

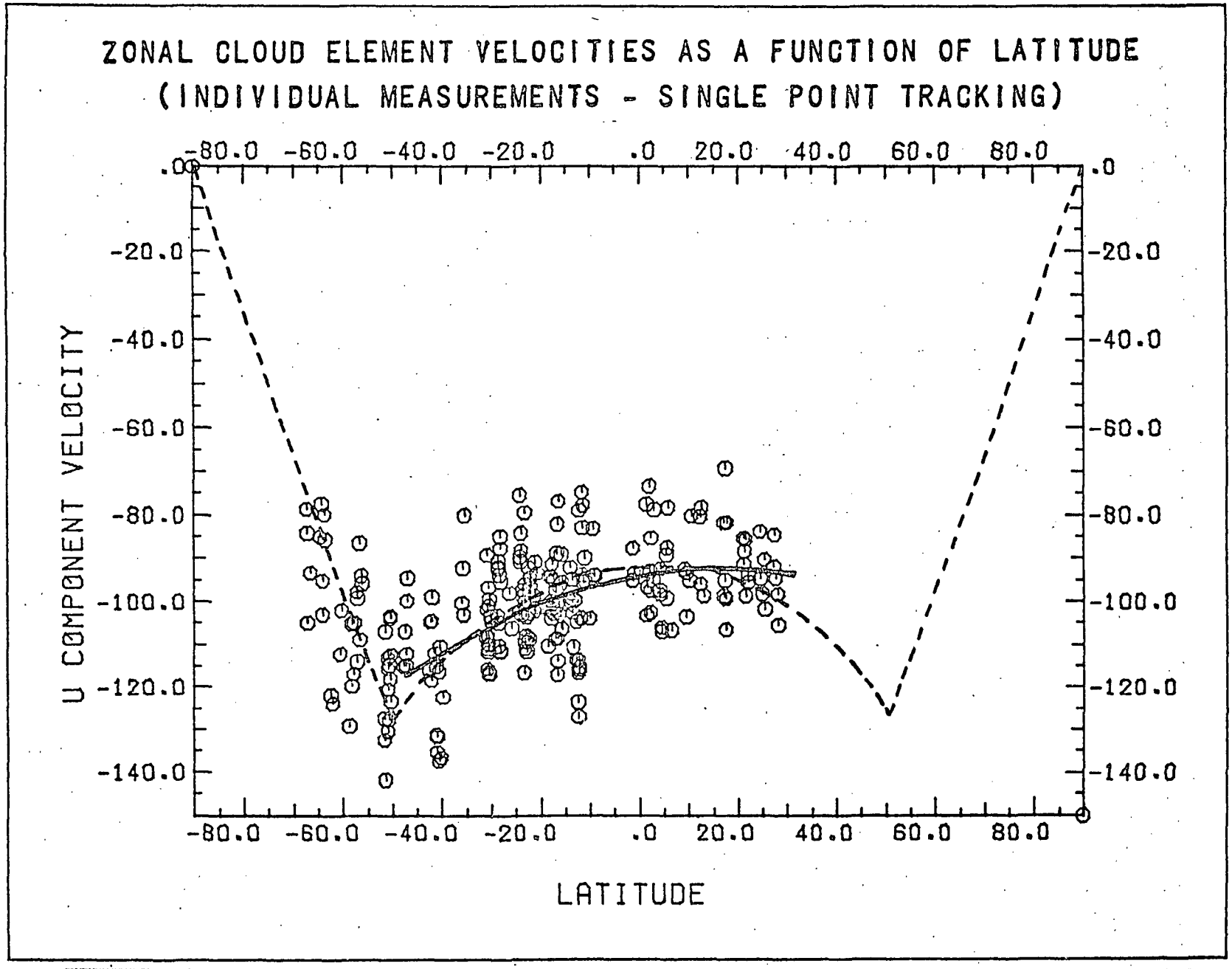

Figure 6b. Single Point Tracking. Scatter plot of 15 m/s edited vectors without target averaging. Dashed and solid lines same as in 6a.

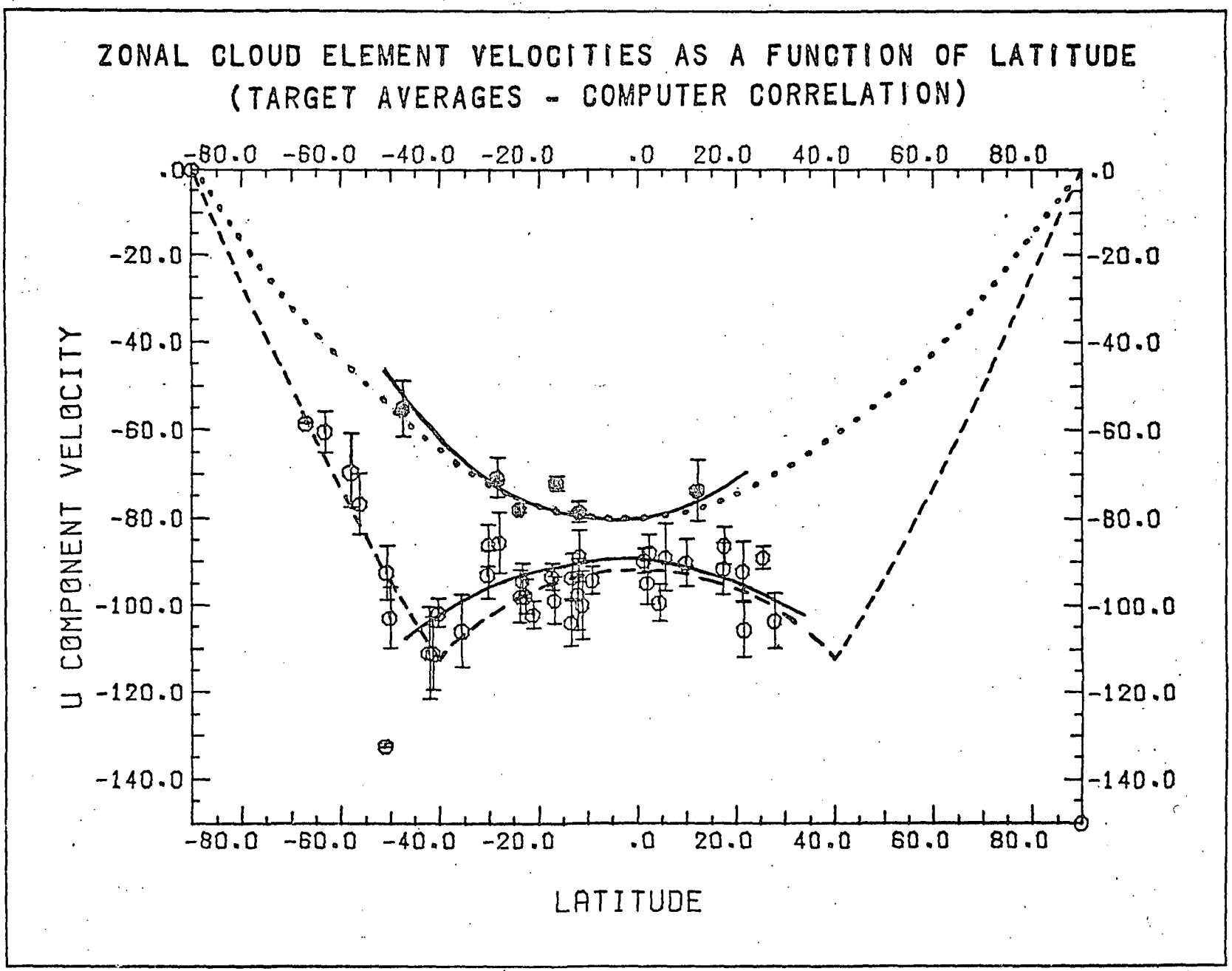

Figure 6c. Computer Measured Vectors. Target averages with RMS Errors indicated. Dashed line is a model having velocity maximum at 40° latitude, with nearly constant angular momentum equatorward and constant angular velocity poleward. The higher velocity solid line is a least squares second order polynomial fit to data points within 45° of the equator. The six targets, lying on the dotted line representing constant angular velocity, are fitted with their own second order polynomial, shown as the lower velocity solid line.

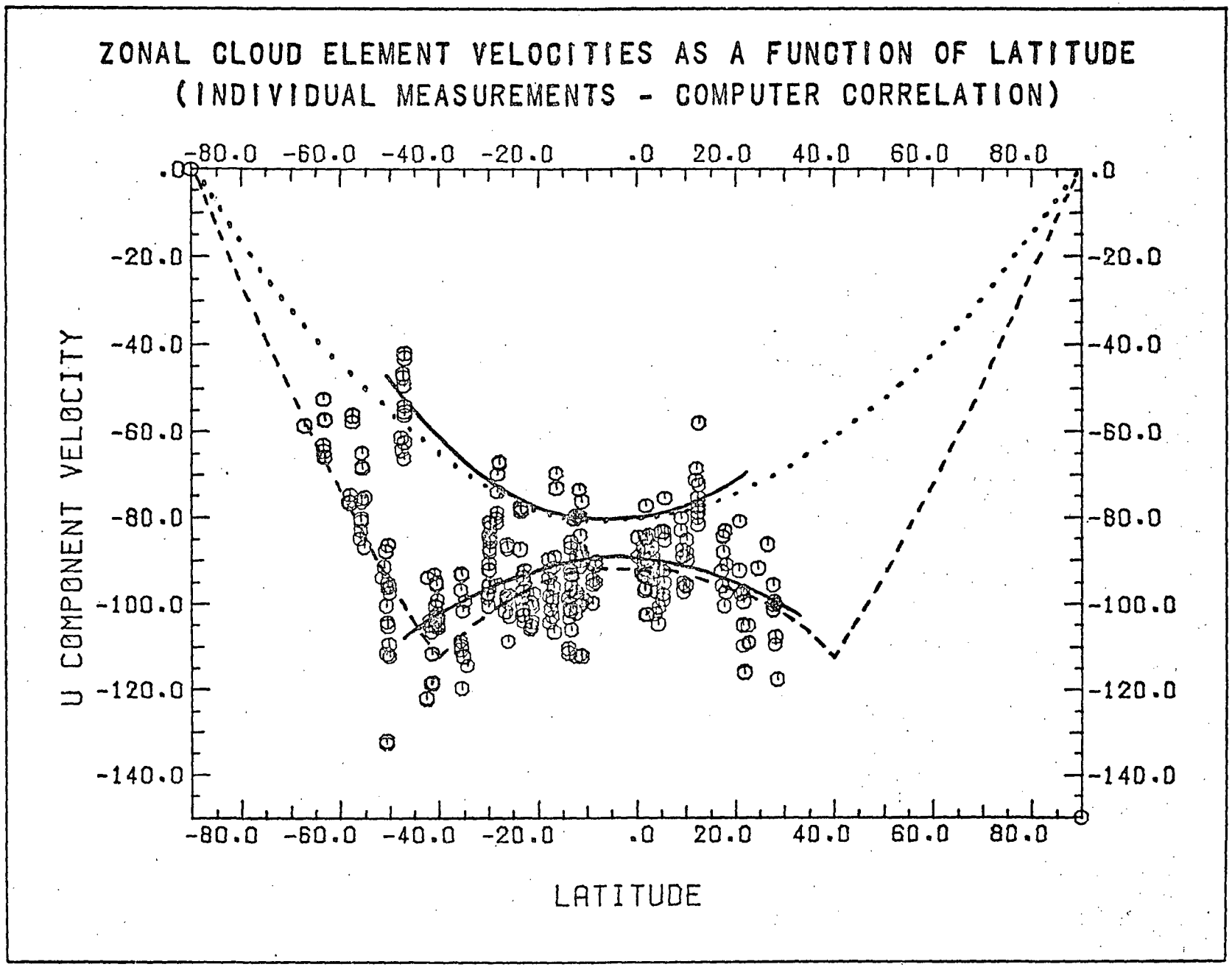

Figure 6d. Computer Measured Vectors. Scatter plot of 15 m/s edited vectors without target averaging. Dashed and solid lines same as in 6c.

TABLE VIII

Summary of Least Squares Fits for Measured Zonal Velocities

VELOCITY MEASUREMENT SET	DISPLAYED IN FIGURE	ZONAL VELOCITY MINIMUM AT LATITUDE	
SP Target Averages	6a	-91.3 m/s	+16°
SP all measurements	6b	-92.1	+12
COMP Target averages	6c	-88.9	-3
COMP all measurements	6d	-89.7	-4
COMP Averages (w/o slow targets)	curve not displayed	-92.3	+3
COMP All (w/o slow targets)	curve not displayed	-92.2	+3

a shape in a time sequence of several frames, is less likely to be affected by edge phenomena. The computer is forced to compare only two data grids and has no other reference frame, such as time continuity.

The differing results of the two measuring techniques, give a potential means of isolating points of constant phase related to wave phenomena, even though a wave may not be structurally coherent or contrasty enough to be seen in the Mariner images. Alternatively, if we are not seeing a wave, the differing results may permit isolating variations in altitude due to shear or changes in cloud structure related to local processes. The further analysis of both higher and lower resolution images (with large numbers of measurements in order to get good statistics) is indicated to identify the exact causes of the observed velocity differences and develop the means to use this technique to advantage. We must understand exactly what is changing and distinguish how the varied measuring techniques respond to such changes.

B. Meridional Motion

The general increase in zonal velocity from the equator to the mid latitudes on Venus is consistent with the simple assumption of conservation of angular momentum, provided some frictional dissipation is allowed. One can say that the zonal velocity profile thereby implies meridional motion. Moreover, the spiral streaks and vortex structure evident in the Mariner 10 images are by themselves strongly indicative of convergent motion toward the poles. Consequently, meridional motion is to be expected. What is surprising is how small it apparently is.

The meridional cloud motions show a correlation with latitude. The velocity tends to be zero near the equator and increases approximately 1.2 m/s in the poleward direction in each hemisphere for every 10 degrees in latitude away from the equator. Figure 7 shows the v-components of the edited measurements, both as target averages (7a and 7c) where the error bars represent RMS deviations in each distinct target average, and as scatter plots (7b and 7d) of all separate measurements. The data points within 45 degrees of the equator were fitted with a least squares straight line, shown solid in each plot. Results are summarized in Table IX.

A comparison with Table VIII shows that the zero crossing in all four plots in Figure 7 occurs at roughly the same latitude as the corresponding minimum zonal velocity in Figure 11. The SP and COMP data sets consistently differ by 20 degrees in where they put the "dynamic equator."

Three targets in 7a and 7c are shown as solid circles. These three should be considered biased since they coincide with the circumequatorial belts. The belts exhibit a southward motion quite anomalous from the other cloud features in that they move much faster (-24 ± 6 m/s) and are organized nearly along lines of constant latitude. They show a brightness maximum about every 12 degrees of latitude, though a filmy structure can be barely discerned between the maxima. The circumequatorial belts are seen only near the equator, only moving south, and only in the period 2-3 days after encounter. Figure 8 shows a scatter plot of SP measurements of the belts made over two 90 minute time intervals. From tables III and IV we would expect 10-18 m/s RMS scatter.

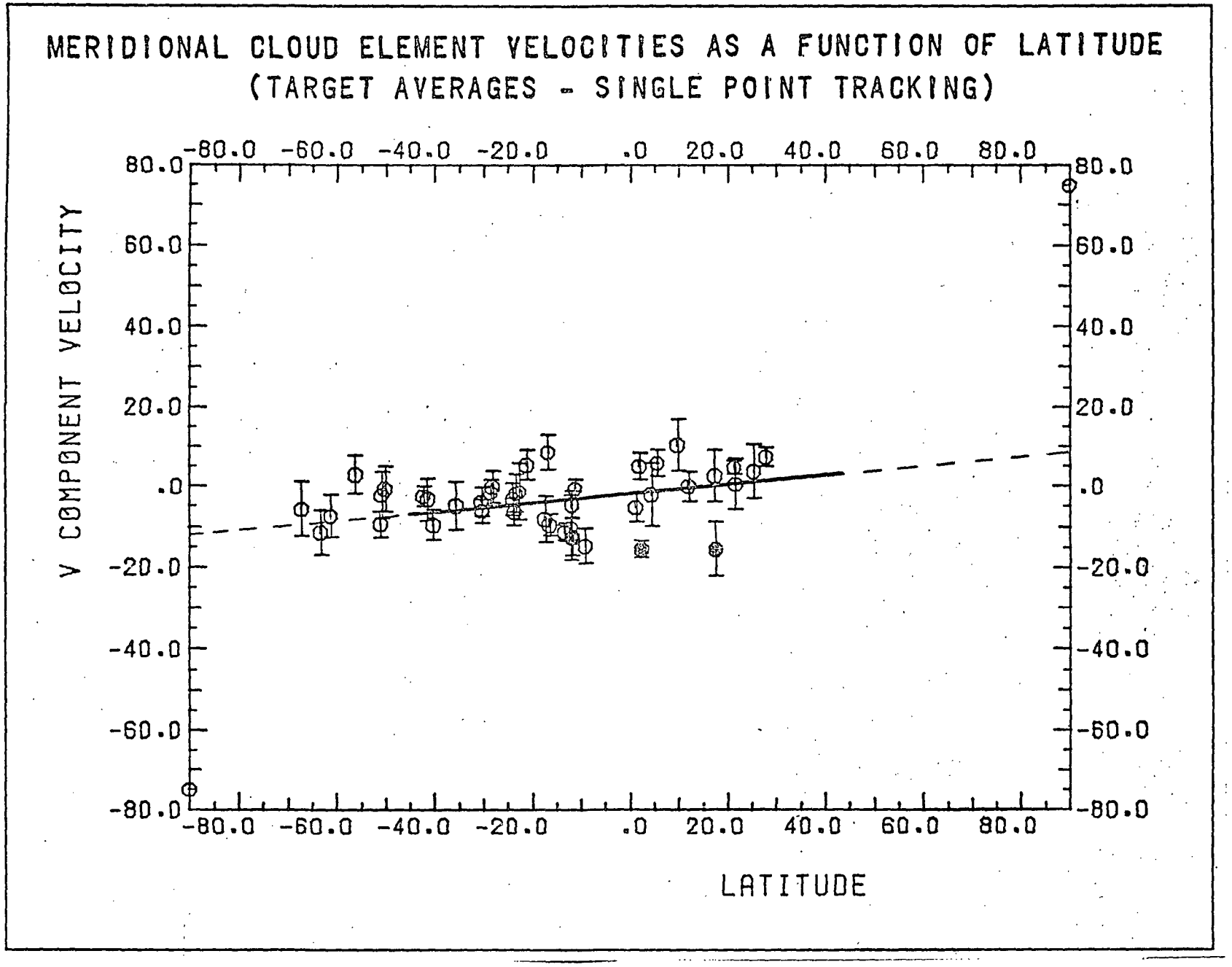

Figure 7a. Single point tracking using 15 m/s cutoff to edit data. Target averages are shown with rms errors. The solid dots are targets coinciding with the circumequatorial belts. The straight line is a least squares fit to the data point.

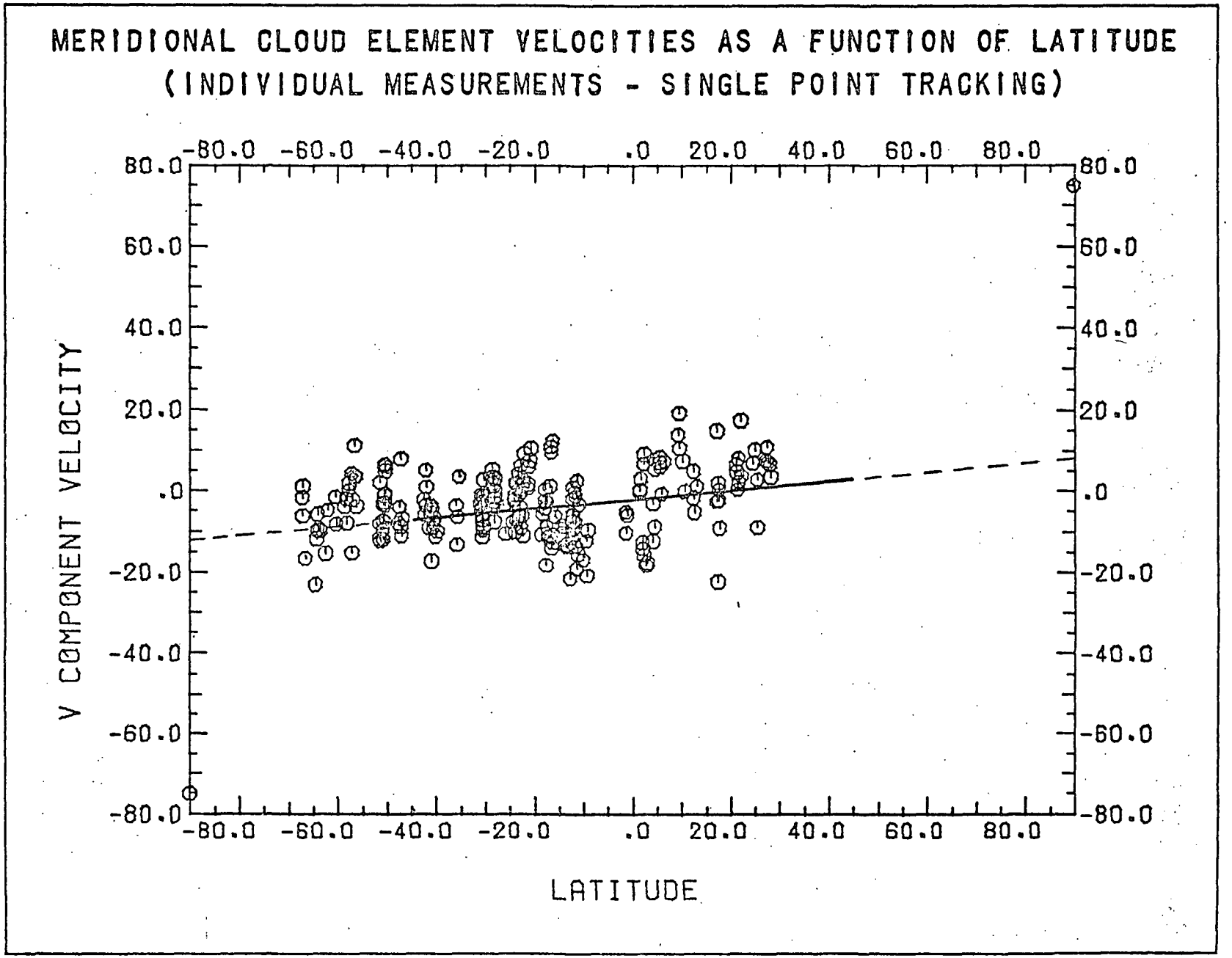

Figure 7b. Single Point Tracking. Scatter plot of 15 m/s edited measurements used to generate target averages in Figure 7a. Linear least squares fit to data points is shown.

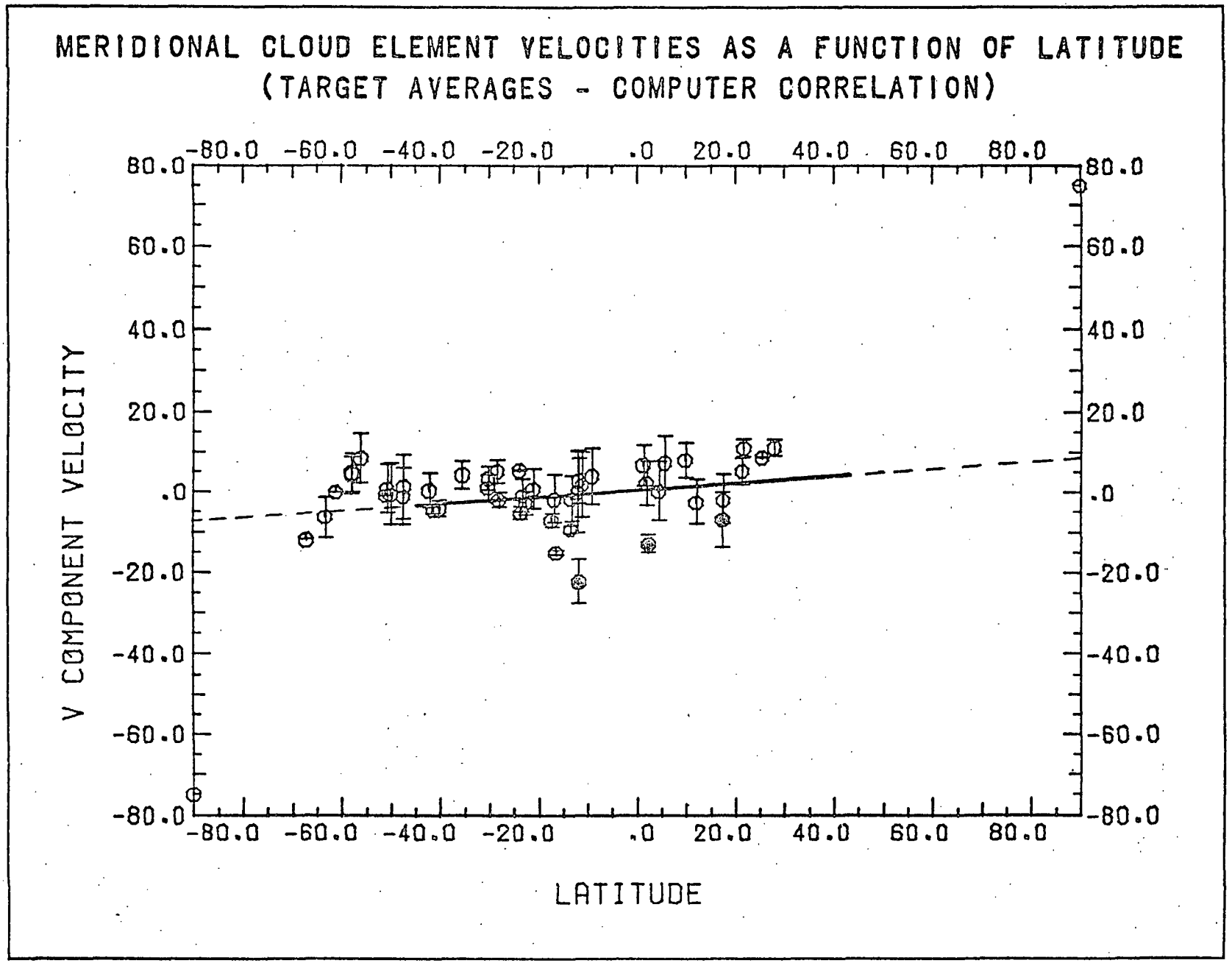

Figure 7c. Computer Measured Vectors. Target averages and rms error are generated from 15 m/s edited data shown in Figure 7d. Solid dots show cloud targets coinciding with circumequatorial belts. Linear least squares fit is also shown.

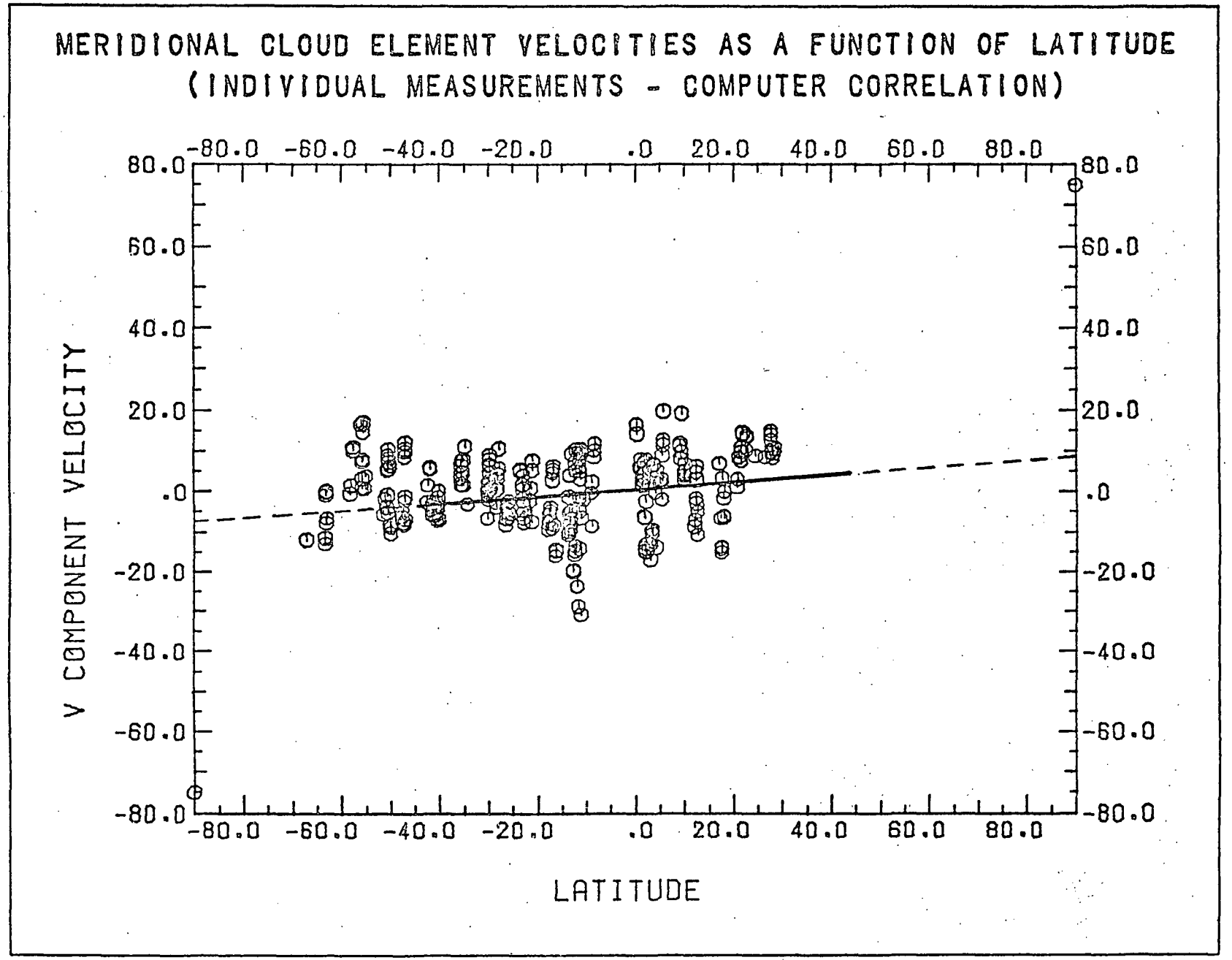

Figure 7d. Computer measured vectors and least squares fit to scatter plot.

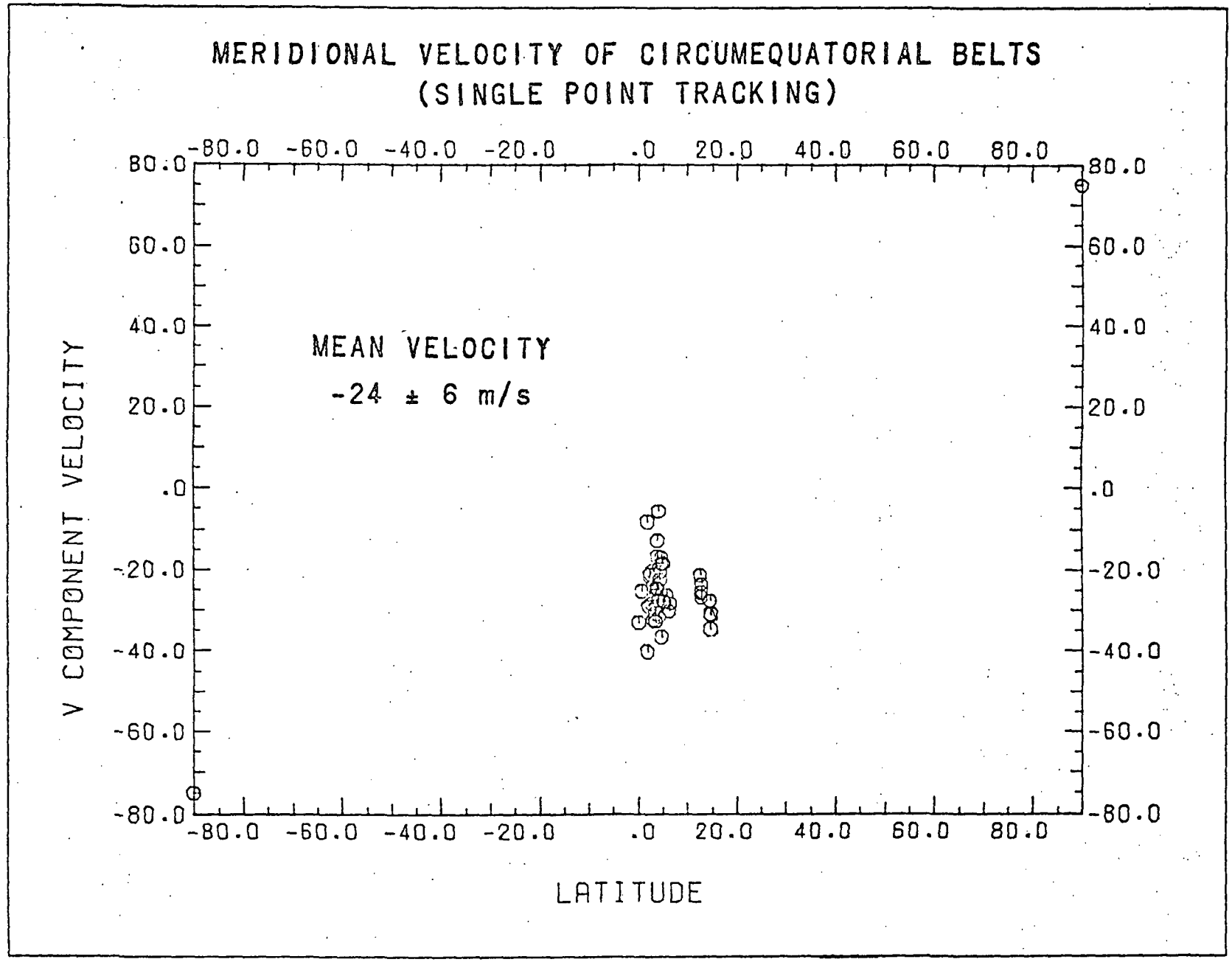

Figure 8. Meridional component of circumequatorial belts as function of longitude. Motion is toward the equator at~20 m/s, as all measurements were made between 0 and 20 degrees north latitude. Belt maxima are about 12 degrees apart in latitude.

TABLE IX

MERIDIONAL MOTION - LEAST SQUARES LINEAR FITS

	Slope	Zero at Latitude
SP Target Averages	.117 m/s/deg.	+17 deg.
SP all Vectors	.133	+12
COMP Target Averages	.103	-7
COMP all Vectors	.102	-8

Returning to Figure 7 one could argue that the northern hemisphere points bias the fitted slopes to somewhat larger values. The southern hemisphere points still exhibit some slope by themselves, however. There is, therefore, a small meridional motion present, and it is definitely not zero.

Note that there is more variance in the measurements at low latitudes (near the subsolar convective region) than in mid latitudes. This may well be due to local "turbulent" fluctuations. Note also that there is far less scatter, and also smaller RMS errors in target means in Figure 7a compared with 6a. We feel that 7a shows what we might reasonably expect to obtain, given the error analysis in Section III. The same scatter and error bar size ought to be present in Figure 6a. Instead, the scatter about the least squares line and the RMS deviations (error bars) for each individual target are considerably larger. Thus, while measurement error and local turbulence might account for some of the scatter in Figure 6a, another phenomenon must also be present. The existence of clouds at different heights moving at different zonal velocitites (vertical wind shear) was strongly suspect at this point, and the results of a search for vertical shear are discussed later.

C. Zonal Velocity Gradient

A correlation is observed between the u-component of the UV cloud motions and longitude such that the lower latitude clouds have a higher velocity. There apparently is a widespread component of zonal acceleration in the direction of motion. One must be careful in interpreting this however, because there is a strong bias in the measurements. Another compelling reason for caution is that models developed to explain the drive for the zonal wind will be influenced by the extent of the measured acceleration effect, its magnitude, and its fluctuation with time. To claim too much at this point could be detrimental to development of a realistic model. Thus, although we feel confident of the measurements of the zonal and meridional wind field to the accuracy stated, the zonal velocity gradient measurements should be treated as a more qualitative observation.

The bias in the correlation plots of Figure 9 can be explained in terms of Figure 5. Notice that because of the tilt of the planet axis with respect to the spacecraft orbit, and because of the lighting conditions at this time, a larger region of observable planet (and hence most of the cloud targets) lies between -20 and -50 degrees latitude and at a lower mean longitude. The mean zonal velocities at these middle latitudes tend to be 10-15 m/s higher

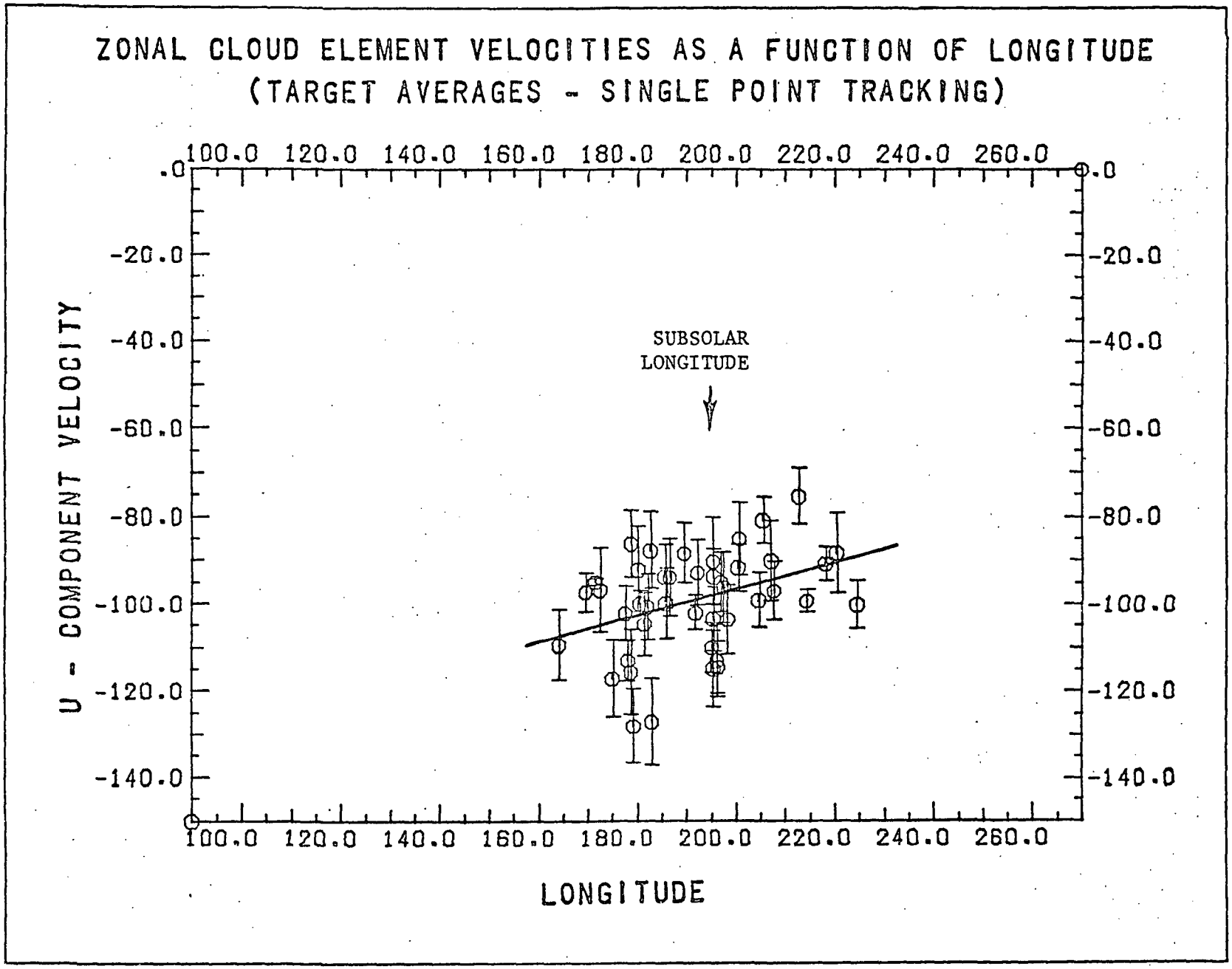

Figure 9a. Zonal wind component of SP measured cloud target averages, with RMS scatter for each target shown as error bars. Slanted line is least squares fit, which may be slanted too much due to the target selection bias mentioned in text. Only latitudes below 45 degrees are included here.

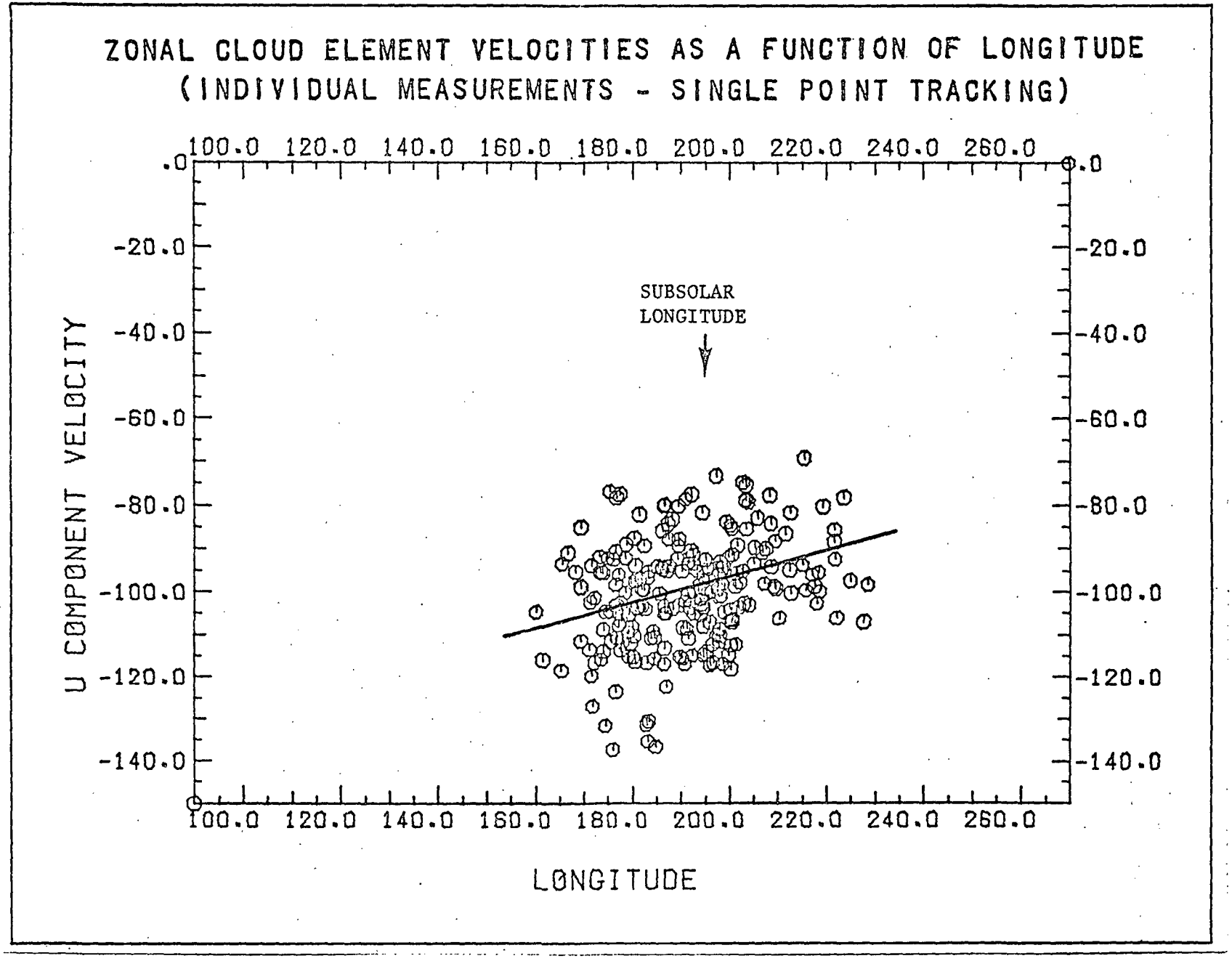

Figure 9b. Scatter plot of individual SP measurements used to generate target averages in Figure 9a.

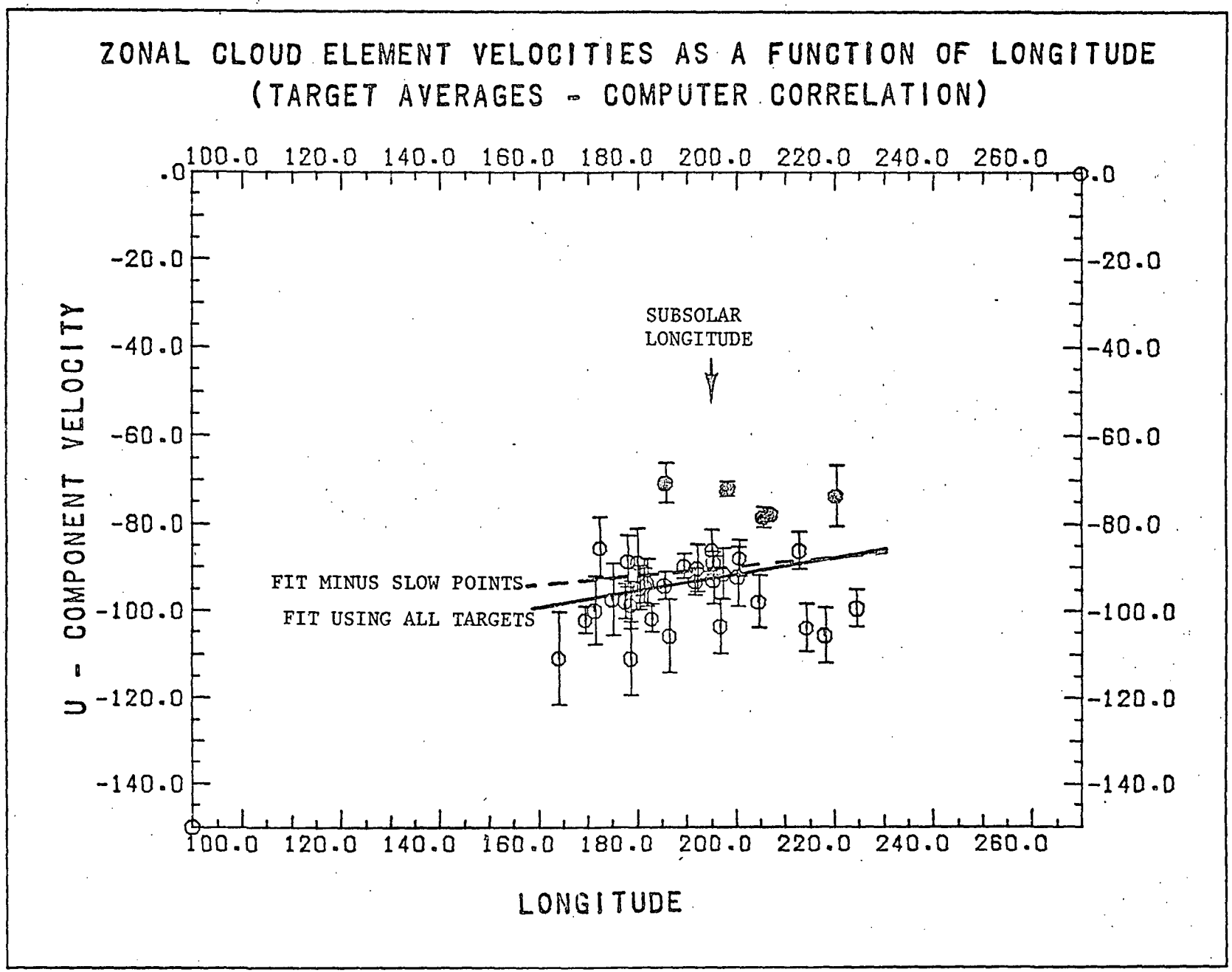

Figure 9c. Computer correlation measurements of zonal wind shown as target averages. Five of the six slow targets are shown as solid dots. A sixth is at a latitude higher than 45°. Least squares fits are shown with and without slow targets.

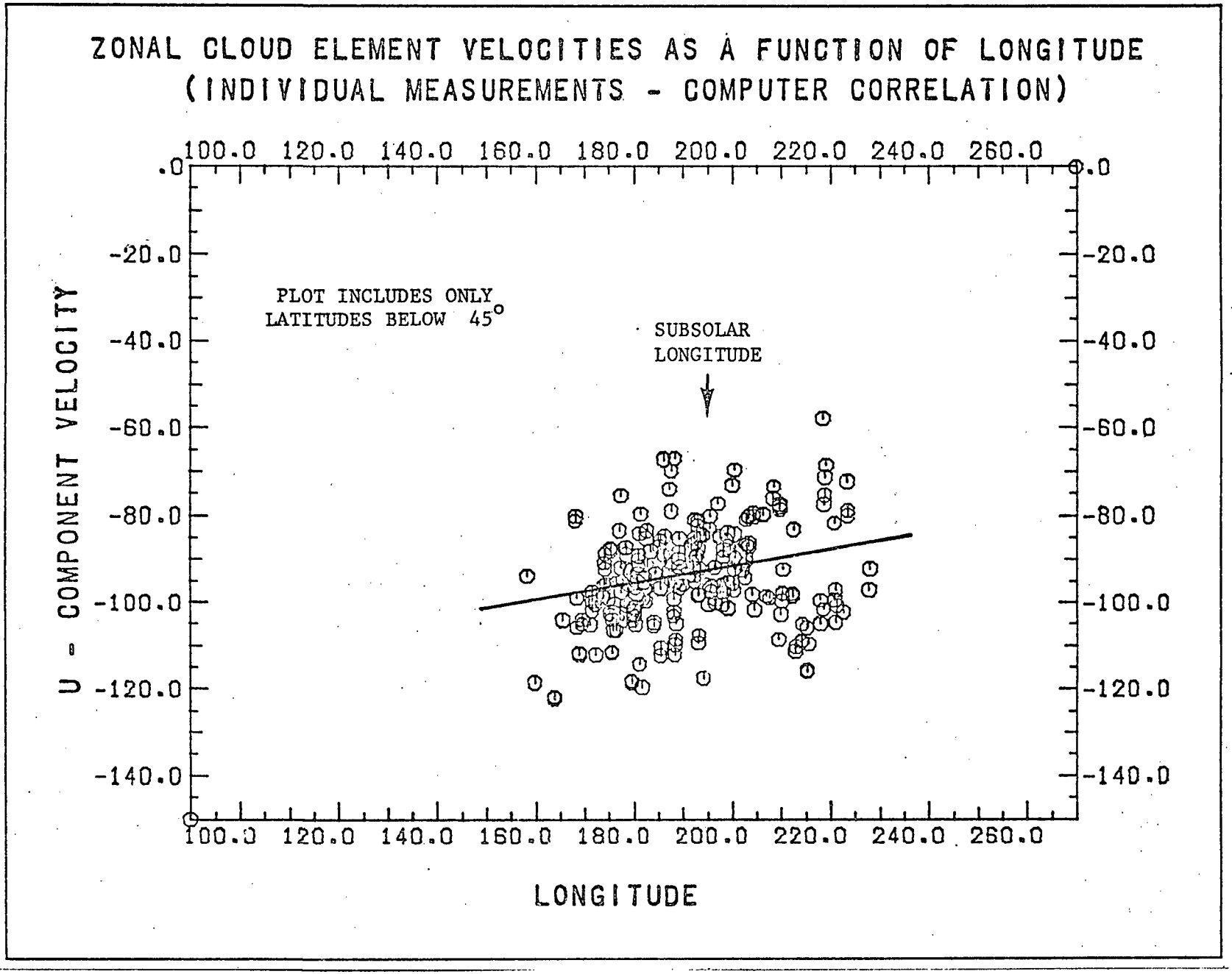

Figure 9d. Scatter plot of measurements used to generate target averages in Figure 9c.

than at the equator, and they would consequently tend to tilt the scatter polts. The data was therefore subdivided into 15 degrees latitude intervals in an attempt to investigate the extent of the bias. Every 15 interval at all latitudes, even poleward of -45 degrees, showed a linear least squares acceleration of 5 to 20 m/s over a latitude range of 220 to 160 degrees. The difficulty, of course, is that when one subdivides into finer and finer data sets the statistics become so poor that the least squares fits don't mean as much. Thus, we claim only that there is a latitudinally widespread zonal velocity gradient present, probably greater than 1-2 m/s over each 10 degrees of longitude. This makes it roughly the same size as the observed meridional velocity gradient. The zonal gradient is not solely limited to the subsolar convective zone, although since all measurements were in regions of solar heating, zonal acceleration could still be sun related. Most important is the fact that, in conjunction with the observed meridional velocity profile, the zonal velocity gradient indicates a widespread divergence centered on the subsolar region.

We must also again note the five "slow" targets discussed earlier and also shown in Figure 9c (the sixth target lies at 47° latitude). These show no indication of participating in any zonal acceleration. This is consistent with the interpretation that they move at constant angular velocity apart from the general fluid flow, and therefore may be wave related or, if not as organized as presently appears, possibly lie at a different altitude relative to the faster targets.

Finally, it should be mentioned that a 5-10 m/s zonal velocity change could account for some of the dispersion in the zonal wind profile. This would add a fourth possible cause for measurement scatter in addition to large scale waves, vertical shear and local turbulent fluctuations.

D. Variation of Meridional Motion with Longitude

There is no observed variation in the v-component with longitude. This effect would be important, since if it existed, it would support the hypothesis of kinetic energy being generated in large amounts in the subsolar convective zone. None of the correlation plots in any and all previously mentioned subdivisions of the data showed more than a total slope of 1-2 m/s. We also see no indication of horizontal wind shear across the spiral streaks, so they cannot be jets. We conclude there is no measureable variation of v with longitude. Any variation which exists is less than 20% of the magnitude of the meridional velocity gradient, and far below the noise level of our measurements.

E. Investigation of Vertical Shear

A detailed search for vertical shear was made in the four 15 km/pixel images to see if this would afford an explanation of why the zonal velocity measurements, shown in Figure 6, had anomalously large scatter compared to both the expected scatter from error analysis and comparison with the measured meridional motions in Figure 7. No convincing evidence was found in the 1 1/2 hour or longer time intervals, but in the 13 minute time interval it was possible to see a few cases where darker blotches evolved in a pattern. The dark spots tended to shrink from the zonally upwind direction and grow zonally

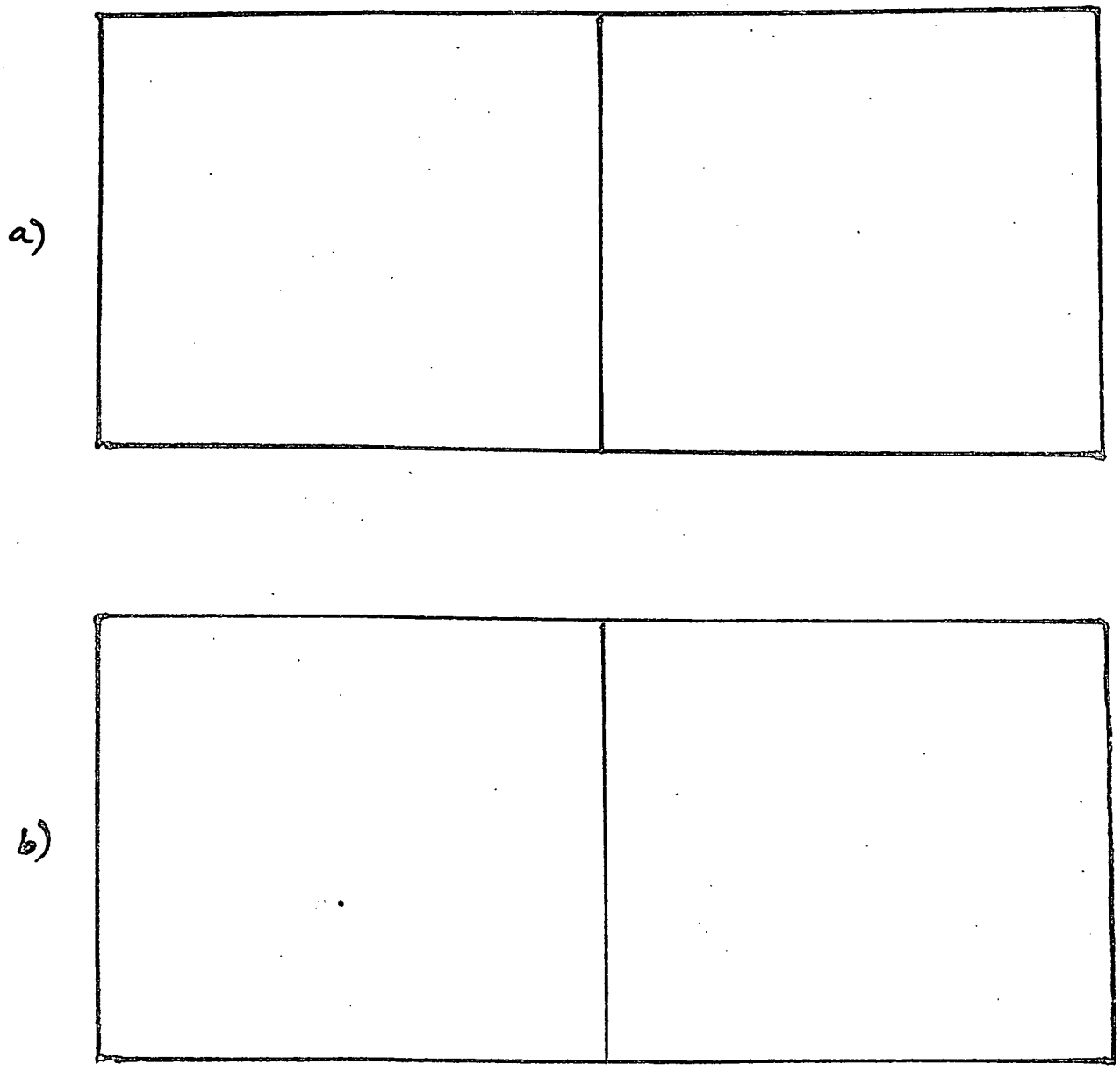

Figure 10. Two examples of vertical shear are shown above in stereo pairs of Mariner 10 pictures made 13 minutes apart. The arrows point to places where bright clouds are covering or uncovering dark patches or other bright clouds at a lower altitude. The upper and faster moving clouds have more parallax and appear closer to the observer in a stereo pair.

downwind as if they were obscured by the lighter features. The changes were barely discriminable in the short time interval, corresponding to relative motions of only a pixel or two, a relative velocity of 15-30 m/s. Once identified in the short time interval, the same features could be seen in the longer time intervals as a change in cloud shape or brightness. Figure 10 illustrates several such features in time sequence.

The darker areas were being obscured by lighter clouds which one can therefore assume to be higher in altitude. Bright patches merged with each other and changed shape and brightness, but showed no such distinct growth pattern. The obscuring bright clouds are partially transparent, since they vary in brightness depending on their background. The higher bright clouds move in the retrograde zonal direction, the same direction as the dark features they obscure, only they move faster. Assuming that the scatter in Figure 7 is due to measurement uncertainty and/or turbulence, and subtracting that from the scatter in Figure 6, one can estimate a shear of 10-30 m/s in the u-component. It must be kept in mind that many of the most deviant u-component measurements were thrown away in the 15 m/s editing process. Consequently the limits of the measured shear may be closer to 0-40 m/s, considering individual cases.

Attempts to measure the shear directly using SP and COMP techniques proved fruitless. The cloud targets could not be tracked well using any technique. They gave widely scattered velocities, although the targets appearing faster to the eye tended to cluster more toward higher velocities. It is likely that instead of two separate velocity fields at two different altitudes, we are observing a continuum of velocities and cloud features over a range of altitudes.

A look at possible causes for the u-component scatter yields the following results:

1. Turbulence - can account for only 1/2 of the scatter in u, and then only if we assume it accounts for all the scatter in v. More likely, some of the v scatter is also due to measurement errors, as our error analysis indicates. Thus, turbulence cannot completely explain the scatter in u.

2. Large Scale Waves - can account for all the scatter if properly organized. Certainly the six wierd cloud targets must be organized by a wave, if anything. They cannot represent mass flow. The chief difficulty with this hypothesis is the fact that except for those six targets, the u-component scatter is, in general, not highly organized, but appears random in character.

3. Longitudinal Acceleration - is simply too small to yield a 15 m/s RMS scatter. At best, the acceleration term amounts to approximately 10 m/s after a cloud has moved 60-80 degrees in longitude. The acceleration ought to be considerably less for any given cloud target in only 3 1/2 hours.

4. Vertical Shear - is the right order of magnitude and is consistent with all the evidence. Shear plus partially transparent clouds could give a mixture of edge velocities, brightness center velocities, and phase velocities whose scatter would vary up to the maximum velocity difference of the shear.

V. CONCLUSION

In this last section, we first summarize the quantitative results of our measurements item by item for easy reference. Then we compare our measurements with those of other experimenters. Finally we give our interpretation of what the measurements mean and indicate where further study could give fruitful results in determining the general circulation regime and dynamical phenomena associated with cloud structure and motions.

A. Summary of Measurements

It is useful to summarize the quantitative results of the measurements before we continue. Remember that all these measurements were made in a 3 1/2 hour period at one point in time, 48 hours after Venus encounter. Considering all the preceding discussion of wave phenomena in sections I and IV, it would be unwise to assume that the velocities themselves are representative of the steady state. Rather, one should consider the structure and organization of the motion fields as the more pertinent information to emerge from these data.

(1) Zonal Flow

a. The mean zonal velocity of small scale cloud elements at the equator is -92 ± 7 m/s, increasing toward higher latitudes with a tendency to conserve angular momentum about the poles.

b. Near 45 degrees latitude, the meridional profile of the zonal wind peaks at a value of -120 ± 10 m/s.

c. Poleward of the zonal velocity maximum is a region of solid rotation with a constant angular velocity of approximately -2.4×10^{-5} r/s.

(2) Meridional Flow

a. A small meridional flow with a mean velocity gradient of 0.12 m/s/deg. is observed, moving from equator to pole in each hemisphere. Scatter in the measurements is too great to determine if the acceleration is constant or varies slightly with latitude.

(3) Longitudinal Velocity Gradient

a. Acceleration of the zonal wind was observed to be present over the entire 60-70° range of longitudes measured, centered on the sub-solar point.

b. Acceleration of the zonal wind was observed to be present over the entire +30° to -60° range of latitudes measured.

c. The magnitude of the zonal velocity gradient is approximately .15 m/s/deg. but could not be precisely measured because of a bias introduced by the viewing geometry.

(4) Vertical Shear

a. Vertical wind shear is present, primarily in the u-component cloud motions, and is observed directly in a few cases and indirectly as velocity measurement scatter with a range generally between 10-30 m/s and an RMS value of about 15 m/s.

b. The shear is at least partially organized in the vertical, since in those cases which can be clearly recognized, the light clouds move faster and both obscure and uncover darker areas, indicating that the zonal wind increases with height. The u-component scatter is slightly more pronounced on the high velocity side of the velocity profiles.

(5) Large Scale Wave Phenomena

a. The circumequatorial belts move south across the equator at -24 ± 6 m/s. Rather than a meridional mass flow or a vertical wind shear, their periodic organization and limited appearance in time argue for interpretation as a wave phenomenon. Insufficient structural detail prevented measurement of the zonal motion of the belts.

b. An 80 m/s (5.5 day period) equatorial velocity appears in a small 6 target subset of the COMP measurements of the u-component. The measurements are organized in such a way as to indicate motion at a constant angular velocity of -1.4×10^{-5} r/s. This velocity is considerably slower than the ~100 m/s (4.4 day period) seen in the large scale "Y" or "Ψ" features in the Mariner 10 data and that of Caldwell (1972). Our -92 m/s cloud velocity at the equator corresponds to a 4.8 day period.

B. Comparison With Other Experiments

Venus has been observed for many years by Earth-based observatories. The motion of the large scale features (the "Y" and "Ψ") have been thoroughly analyzed. Results were reported by Smith (1967), Dollfus (1968), and Boyer & Guerin (1969). There seems to be general agreement that the speed of the large UV features is about 90 to 110 m/s, corresponding to a rotation period of 4 to 5 days. The wide variation of the measured periods indicates, however, that the markings may vary in speed or shape from time to time. More recent work reported by Caldwell (1972) from Planetary Patrol observations gives 4.41 days as the rotation period of the "Y" and suggest variations in velocity and cloud altitude as a possible reason for the discrepancy between the earlier observations.

Scott and Reese (1972) point out that there is a bimodal distribution of measured rotation periods and that a shorter period of 4.06 days, although most dominant, can be explained on the basis of a commensurability between the 1 day period of Earth and the assumed 4 day period of the Venus clouds, whenever all the observations are made from a single observatory. This lends more credence to the 4.59 day period they mention, the 4.41 days of Caldwell, and the 4.7 days of Smith. If, indeed, the large scale features are coupled to a fluctuation in altitude or velocity or some other parameter which varies along with the intensity of the "Y", or are coupled to a wave which triggers convection or alters the cloud optical properties or shape of the "Y", a slight variation about a 4.5 day mean measured period is not unreasonable. A period of 4.6 ± 0.2 days would fit most of the observations, including ours. A distinction must be made, however, between motion of large scale, telescopically observed features, which could be wave related, and motion of small scale cloud elements, which are more likely to correspond to true mass motion.

Particular attention should be given to results of measurements performed by Sidi (1975) using a stereoscopic comparator technique on Mariner 10 hard copy images. The Sidi measurements cover a similar time interval to ours and overlap with ours by 50%, although none of the frames used are exactly the same. One would thus expect the measured velocities to be the same in both cases, and they are indeed quite similar.

Sidi finds increasing zonal velocity at higher latitudes, tending toward conservation of angular momentum about the poles. The mean equatorial velocity is -82 m/s east of the subsolar point and -82 to -110 m/s toward the west. A transition longitude passing through the subsolar point sharply divides the accelerated from the unaccelerated zonal flow. The magnitude of the acceleration Sidi found is 0.48 m/s/deg., compared with our ~0.15 m/s/deg. averaged across the disk with no sharp transition longitude observed. It should be noted that Figure 9, especially 9c and 9d, could be in agreement with Sidi.

Sidi also finds an "equatorial belt" moving 5 m/s slower than the zonal flow, with meridional velocity toward the equator (probably the "circumequatorial belt" mentioned here and in Murray, et.al. (1974), although the terminology used by Sidi is somewhat confusing), and a perfectly spherical appearing polar region (with no bumps or hollows) therefore implying solid body rotation. Meridional velocities are small, <10 m/s everywhere, and generally moving from equator to poles with no obvious organization. We have noted a tendency for the meridional velocities to increase at higher latitudes, but in all other respects, Sidi's observations agree reasonably well with ours.

Boyer (1973) measured the velocity of the "Y" and "Ψ" features in Earth-based photos of Venus and obtained faster velocities near the evening terminator. The "morning" average zonal velocity was -83 m/s while the "evening" average zonal velocity was -122 m/s. It should be noted that Boyer's velocities are again for larger scale features and thus not directly comparable with the measurements of Sidi and our own, both of which rely on small details in the clouds. On the other hand, there exist velocity

measurements of Traub and Carleton (1975) based on spectroscopic Doppler shifts which yield similar gradients: -73 m/s in the "morning" and -111 m/s in the "afternoon". The zonal variation in velocity thus appears to be very real, and also apparently sun-locked and visible at all scale sizes on Venus from global scale to molecular.

The question of meridional motion is somewhat more confused. If we believe with Traub and Carleton that there is at least occasionally a substantial CO_2 flow toward the equator, the situation becomes much more complex than indicated by our measurements. Traub and Carleton allude, in fact, to the possibility of multiple cloud layers and vertical wind shear. Everyone who has seen the circumequatorial belts in the Mariner 10 images agrees they can move toward the equator, and there is no proof that they represent only wave motion and not mass motion. The higher resolution Mariner 10 pictures may permit resolving some of the confusion by giving us a better look at vertical structure in the UV clouds.

C. Conclusions

In light of the foregoing discussion, it is evident that one should be extremely cautious in believing too literally in any number representing a velocity or period. Rather, our measurements should be considered as giving greater insight into the structure and organization of the upper atmosphere dynamics. It is on this point we ought to place the emphasis.

1. The zonal flow on Venus above 60 km altitude, is organized like a vortex, as first explained by Suomi (1975). There is a slow meridional flow from equator to pole in each hemisphere and a tendency for the zonal flow to conserve angular momentum about the poles, but with a slight frictional loss. The result is that we find differential rotation of the upper atmosphere at low latitudes and solid rotation at high latitudes, with a transition region near 45° latitude.

   That this is mass motion and not a wave is evident from the velocity profiles and the correlation with spectroscopic Doppler shifts in CO_2 absorption lines. We can also infer from the amount of angular momentum present that this vortex could be perturbed, but is likely to be structurally stable over periods of days or weeks. As a result, the upper level global energy transport is most like a modified Hadley cell, and we would expect from the evidence of the Venera probes and the Mariner 5 & 10 radio occultation results to find considerable vertical dynamic structure on Venus below 60 km altitude.

2. Evidence of zonal velocity perturbations is strong. The zonal flow is faster toward the evening terminator, according to most recent observations, and shows up in both small scale and large scale features. Whether this acceleration is due to a solar tide, a global scale wave, Reynolds stresses, or some other phenomenon is unexplained. We can be reasonably sure that it occurs in a wide band at least 20° each side of the equator, and may extend

to even higher latitudes. It is hard to escape the fact that the sun strongly influences the upper atmosphere dynamics, and probably in a very direct way, as opposed to indirectly by merely supplying energy. On the other hand, there seem to be no large horizontal pressure gradient forces generating jets or large meridional flow. The emphasis is more on a steady or periodic influence of the sun in the zonal and vertical dimensions only.

3. Some evidence of vertical shear in the zonal flow is evident, with higher clouds travelling faster and obscuring lower features, both light and dark. Error analysis reveals that this u-component shear probably appears as a major component of the scatter in the zonal cloud velocity measurements. Coupled with the low meridional velocities, this vertical shear is evidence for a global dynamic balance similar to geostrophic flow on Earth. One must find another inertial force, however, for the coriolis force on Venus is too small to balance a meridional pressure gradient of even a few millibars.

4. The picture of waves on Venus is very confused. We mentioned in the introduction that the small lapse rate of temperature above 60 km tends to give the atmosphere great vertical stability. This inhibits convection, and also provides a strong restoring force to damp out vertical perturbations. These conditions are very conducive to wave motion, and we must therefore pay a good deal of attention to wave motions as a possible means of transport of energy and momentum. This complicates the dynamic picture considerably, since no unambiguously clear interpretation of the dynamics can be made without proof that waves are not present. Unfortunately, all the proof is in the other direction. We see evidence of waves all over the place.

   The "Y" features are wavelike in that they are coherent in time over periods of 5-10 revolutions in the presence of a differentially rotating mass field. The spiral streaks are wavelike in that they move with the mass field but are at least semi-periodic along lines of constant latitude, especially near the equator. The circumequatorial belts are wavelike, being periodic in the meridional direction and appearing only at certain times and moving in certain directions. The bowlike waves appear in pairs and only at certain times. The bright polar band "nutates" with a 4-5 day period. There are periodic variations in the intensity of CO_2 absorption in the upper atmosphere. The one consolation in all of this is that the vortex motion of the mass field seems unaffected to first order. Venus looks in the Mariner 10 pictures like it usually does from Earth.

There are bright aspects to consider too, however. It appears that we can measure second order effects (~10 m/s) in the velocity field. Moreover, because Venus appears so inhomogeneous in the UV images of Mariner 10, there is a wealth of detail to study in a quantitative way. We can extend the velocity measurements over several more days, paying particular attention

to variations and eddy components. We can study the obvious inhomogeneities and vertical structure and shear present in the closeup high resolution data. Moreover, we can use the measured velocity fields to provide boundary conditions for theoretical models, thereby limiting the range of "reasonable" conditions which have to be considered.

It is overwhelmingly clear, from this first look at the Mariner 10 data, that we have an exceedingly complex and variably structured data set. On the other hand, the many pictures, taken over almost the entire range of time and space scales on which the atmosphere is evolving, permit a glimpse into practically all the dynamic interactions short of climatological change. The Pioneer Venus orbiter will give us a long time base in a couple years, while the atmospheric probes should give insight into the vertical structure and deep layers. The prospects for finding out more about the atmosphere of Venus have never looked brighter. There is much interesting work ahead.

ACKNOWLEDGEMENTS

We gratefully acknowledge the help of the staff at the Jet Propulsion Lab for their aid in obtaining and processing the image data tapes and the care and attention to the myriad small details which have made our work easier. In particular we wish to thank Ed Danielson, Bob Toombs, and Ken Klassen for their contributions as imaging team representatives and also Jim Soha and Don Lynn of the Image Processing Lab for their help in data preparation.

The McIDAS system at the Space Science and Engineering Center was built with ideas from many sources, but its power and versatility is the result of the creative combination of talents of four people: Terry Schwalenberg, hardware design and construction; John Benson, systems programming; Dennis Phillips, navigation and correlation algorithms; and Eric Smith, applications programming. Image alignment was done by Gary Chatters. Some of the plotting routines were written by Bruce Knaack. Special mention should be given to Sanjay Limaye for the excellent job he has done in the tedious task of reseau measuring, and for his aid in helping to navigate the images. Finally, we wish to thank Nancy Kitzman for her usual excellent care and attention to detail in typing of the final manuscript.

This research was supported by JPL Contract #953034.

BIBLIOGRAPHY

Barker, Edwin S.; 1975: "Comparison of Simultaneous CO_2 and H_2O Observations of Venus," J. Atmos. Sci., 32, 1071-1075.

Boyer, C.; 1973: "The 4-day Rotation of the Upper Atmosphere of Venus," Planet Space Sci., 21, 1559-1561.

Boyer C. and Guerin, P.; 1969: "Etude de la Rotation Rétrograde, en 4 Jours, de la Couche Exterieure Nuageuse de Vénus," Icarus, 11, 338-355.

Caldwell, John; 1972: "Retrograde Rotation of the Upper Atmosphere of Venus," Icarus, 17, 608-616.

Coffeen, David L.; 1971: "Venus Cloud Contrasts," Planetary Atmospheres, Sagan, et.al., Eds., Reidel, 84-90.

Deveaux C.; Herman, M.; and Lenoble, J.; 1975: "Interpretation of the Photometric Measurements of Venus by Mariner 10," J. Atmos. Sci., 32, 1177-1189.

Dollfus, A.; 1968: "Synthesis on the Ultraviolet Survey of Clouds in Venus' Atmosphere," The Atmospheres of Venus and Mars, J. Brandt and M. McElroy, Eds., Gordon and Breach, 133-144.

Hansen, J.E.; and Hovenier, J.W.; 1974: "Interpretation of the Polarization of Venus," J. Atmos. Sci., 31, 1137-1160.

Hapke, Bruce; 1975: "Mariner 10 Photometry," The Atmosphere of Venus, NASA SP-382, 69-76.

Howard, H.T., et.al.; 1974: "Venus: Mass, Gravity Field, Atmosphere, and Ionosphere as Measured by the Mariner 10 Dual Frequency Radio System," Science, 183, 1297-1301.

Lacis, A.A.; 1975: "Cloud Structure and Heating Rates in the Atmosphere of Venus," J. Atmos. Sci., 32, 1107-1124.

Marov, M. Ya.; 1972: "Venus: A Perspective at the Beginning of Planetary Exploration," Icarus, 16, 415-461.

Murray, Bruce C., et.al.; 1974: "Venus: Atmospheric Motion and Structure from Mariner 10 Pictures," Science, 183, 1307-1315.

O'Leary, Brian; 1975: "Venus: Vertical Structure of Stratospheric Hazes From Mariner 10 Pictures," J. Atmos. Sci., 32, 1091-1100.

Pollack, James B., et.al.; 1975: "A Determination of the Composition of the Venus Clouds from Aircraft Observations in the Near Infrared," J. Atmos. Sci., 32, 1140-1150.

Prinn, Ronald G.; 1975: "Venus: Chemical and Dynamical Processes in the Stratosphere and Mesosphere," J. Atmos. Sci., 32, 1237-1247.

Sidi, C.; 1976: "Stereoscopic Observations of Winds on Venus," Preprint, submitted to Icarus.

Soha, J., et.al.; 1975: "IPL Processing of the Mariner 10 Images of Mercury," J. Geophys. Res., 80, 2394- .

Scott, A.H. and Reese, E.J.; 1972: "Venus: Atmospheric Rotation," Icarus, 17, 589-601.

Smith, B.A.; 1967: "Rotation of Venus: Continuing Contradictions," Science, 158, 114-116.

Suomi, Verner; 1975: "Cloud Motions on Venus," The Atmosphere of Venus, NASA SP-382, 42-58.

Traub, W.A. and Carleton, N.P.; 1975: "Spectroscopic Observations of Winds on Venus," J. Atmos. Sci., 32, 1045-1059.

Travis, L.D.; 1975: "On the Origin of Ultraviolet Contrasts on Venus," J. Atmos. Sci., 32, 1190-1200.

Young, A. T.; 1973: "Are the Clouds of Venus Sulfuric Acid?," Icarus, 18, 564-582.

Young, Andrew T.; 1975: "The Clouds of Venus," J. Atmos. Sci., 32, 1125-1132.